Lithos 132-133 (2012) 113–126

Contents lists available at SciVerse ScienceDirect

Lithos

journal homepage: www.elsevier.com/locate/lithos

Geochemistry of mafic dykes from the Southeast Anatolian ophiolites, Turkey: Implications for an intra-oceanic arc–basin system

Ali Riza Colakoglu [a,*], Kaan Sayit [b], Kurtulus Günay [a], M. Cemal Göncüoglu [c]

[a] Yüzüncü Yil Üniversitesi, Jeoloji Mühendisligi Bölümü, Zeve Kampüsü, TR-65080 Van, Turkey
[b] Department of Geological Sciences, San Diego State University, San Diego, CA 92182-1020, USA
[c] Middle East Technical University, Department of Geological Engineering, 06531, Ankara, Turkey

ARTICLE INFO

Article history:
Received 12 March 2011
Accepted 26 November 2011
Available online 4 December 2011

Keywords:
Southern Neotethys
Ophiolite
Diabase dyke
SSZ
OIB

ABSTRACT

The Late Cretaceous–Tertiary accretionary prism in Eastern Turkey includes several ophiolitic megablocks and/or tectonic slivers (Mehmetalan, Mollatopuz and Alabayir) within a mélange complex, mainly comprising harzburgite, dunite and cumulate-textured gabbro. The diabases, which are the main focus of this study, cut across the ophiolites as parallel and variably thick dyke-swarms. Geochemistry of the diabases reveals three distinct groups, including a) supra-subduction zone (SSZ) type, which is characterized by marked Nb-anomaly and normal mid-ocean ridge basalt (N-MORB) like HFSE distribution, b) enriched MORB (E-MORB) type, showing some degree of enrichment relative to N-MORB, c) oceanic-island basalt (OIB) type with characteristic hump-backed trace element patterns, coupled with fractionated REE distribution. Among these groups, SSZ- and E-MORB-type signatures are acquired from the Mehmetalan and Mollatopuz suites, whereas OIB-type characteristics are found in the Alabayir suite. The melting models indicate involvement of both depleted and enriched sources for the genesis of the studied dykes. The close spatial relationship, similar ages (based on Ar–Ar dating) and the presence of variable subduction component displayed by Mehmetalan and Mollatopuz suites may indicate melt generation in an intra-oceanic SSZ within the southern branch of Neotethys. In spite of the solely OIB-like character of the Alabayir suite, the similar age obtained from these dykes may suggest their formation in a similar SSZ setting. Alternatively, the Alabayir suite may have represented an oceanic island or seamount formed in an intra-plate setting with or without plume influence. We suggest that decompression melting triggered by slab roll-back mechanism during the closure of the southern branch of the Neotethys during the Late Cretaceous may have been the main process that led to generation of magmas of both depleted and enriched characteristics.

1. Introduction

Ophiolites are the relicts of ancient oceanic lithosphere that are found along orogenic belts. Owing to tectonic processes operating during the closure of oceanic domains, the oceanic lithosphere is disintegrated into fragments of variable sizes. During accretion, the chaotic mixing of these fragments leads to formation of an ophiolitic melange in which the relicts of oceanic lithosphere are found as dismembered pieces. Within melange complexes including such dismembered bodies, it is not always the case that one can find the whole succession of ophiolite. Even though the individual pieces can provide a part of its respective oceanic realm, the detailed examination of each body, and the integration of the individual pieces into a whole may help solve the puzzle, and can provide invaluable information about the main picture, that is the geodynamic evolution of the ancient oceanic realm.

The Neotethys, which is one of the ancient Tethyan oceanic realms believed to have existed between Triassic?–Late Cretaceous, is of particular importance, since it includes numerous ophiolitic bodies which seem rather absent in its pre-Triassic representatives (e.g. the Palaeotethys). Therefore, the Neotethys bears a good deal of evidence inherited from oceanic lithosphere, which in turn allows us to examine the nature of oceanic crust and the tectonic setting which it came from. In spite of the fact that the ophiolites can form in a number of tectonic settings, including mainly mid-ocean ridges, island arcs, and back-arcs (e.g. Bortolotti et al., 1996; Pearce et al., 1981; Robertson, 2002), there is now a growing evidence that Neotethyan ophiolites display generally SSZ-type characteristics (e.g. Aitchison et al., 2000; Ahmad et al., 2008). In terms of Neotethyan events, Anatolia is a critical place to examine, since the ophiolitic relicts inherited from the closure of the Neotethys are preserved along the suture zones within the Anatolian borders.

It is commonly accepted that Anatolia is made up of several microcontinental blocks seperated by suture zones related to the Paleo- and Neotethys (Göncüoglu et al., 1997; Robertson and Dixon, 1984; Sengör and Yilmaz, 1981). From these, the multi-

* Corresponding author. Tel.: +90 432 2251024 2964; fax: +90 4322251732.
E-mail address: arc.geologist@yyu.edu.tr (A.R. Colakoglu).

0024-4937/$ – see front matter © 2011 Elsevier B.V. All rights reserved.
doi:10.1016/j.lithos.2011.11.023

armed Neotethys Ocean is relatively well-documented in west and north Anatolia. In east Anatolia, however, there is yet no consensus on the distribution of the continental microplates, nor on the location and number of the suture belts (e.g. Colakoglu and Arehart, 2010; Parlak et al., 2004, 2009; Robertson, 2002; Robertson et al., 2006; Yilmaz, 1993; Yilmaz et al., 1987). This is mainly due to a very thick cover of Neogene–Quaternary volcanic-volcanosedimentary rocks that obscure the distribution and relations of pre-Neogene rock-units. Overall, the ophiolitic rocks between Erzurum and the Armenian Border (Fig. 1) are commonly considered as members of the northern Neotethyan ophiolites of the Ankara-Erzincan Ocean. The origin of a number of ophiolitic outcrops and metamorphic assemblages between the Persian border to the east of Van Lake and the better-known ophiolites and crystalline rocks in Malatya–Elazig area in the west (Fig. 1), however, is a matter of debate (e.g. Elmas and Yilmaz, 2003; Robertson et al., 2007). The critical discussion (for details see Robertson, 2006) being whether they are derived from the Ankara-Erzincan Ocean, or whether they are located on the eastern continuation of the Mus branch of the southern Neotethys of Sengör et al. (2008) or alternatively the Amanos–Elazig–Van Suture Belt of Göncüoglu et al. (1997) and Göncüoglu (2010).

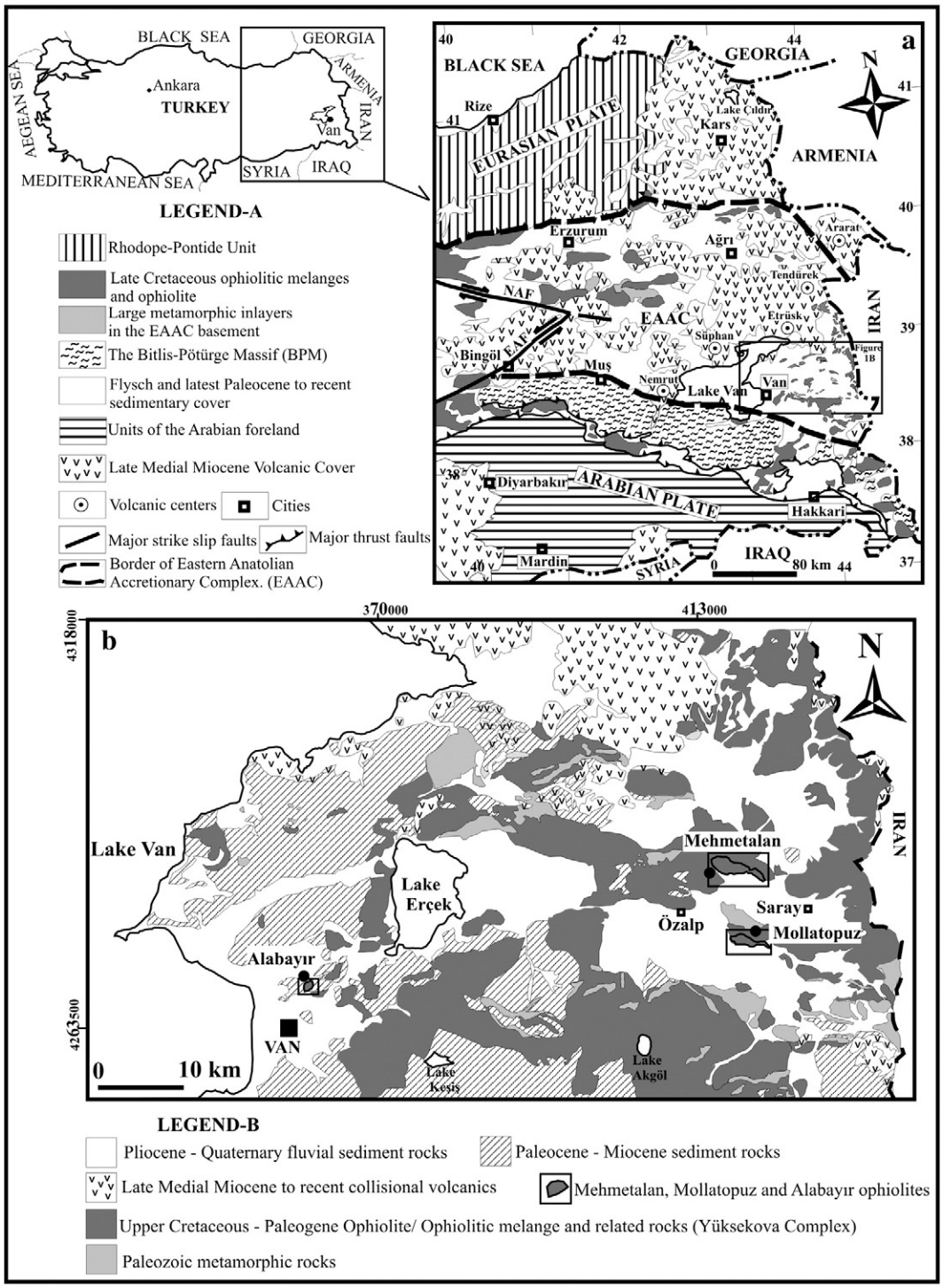

Fig. 1. A — Simplified geological map of the Eastern Anatolia (modified from Keskin, 2005). B — Geological map of the area to the east of Lake Van (modified from MTA, 2007).

The main subject of this study is the geology and petrology of the isolated diabase dykes in Mehmetalan, Mollatopuz and Alabayir ophiolites that are situated to the east of Lake Van. The ophiolitic rocks are observed as relatively large tectonic units in a melange-complex named as the Eastern Anatolian Accretionary Complex (EAAC, Sengör and Yilmaz, 1981), representing the remnants of the southern Neotethys. We here document the evidence for generation of at least some of these dykes in intra-oceanic SSZ-type setting, and their implications with respect to the other Neotethyan ophiolites.

2. Geological framework

Burried under the Neogene and Quaternary volcanic-volcaniclastic cover, the EAAC to the east of Lake Van (Fig. 1b) is composed of the Eocene–Oligocene flysch (Kirkgecit Formation) with olistoliths and/or tectonic lenses of an ophiolitic melange (Yüksekova Complex) and metamorphic rocks (Acarlar et al., 1991; Ketin, 1977; Senel and Ercan, 2002). The main body between the Lake Van and the Iranian border is characterized by imbricated flysch deposits that become younger from north to the south. The Yüksekova Complex comprises lithologies of a dismembered ophiolitic succession and an island arc together with oceanic sediments (Perincek, 1990; Yilmaz, 1993). The metamorphic rocks are partly metavolcanics of the Yüksekova Complex, also known as the Mordag Metaophiolites in the southeast of Van (Elmas and Yilmaz, 2003; Perincek, 1990). Less frequently, recrystallized limestones and quartzites, resembling the Paleozoic rocks of the Tauride–Anatolide basement are encountered. The available fossil data from the oceanic sediments in the Yüksekova Complex in east of Van suggests a Late Cretaceous–Early Paleocene depositional age (Elmas, 1992; Göncüoglu and Turhan, 1984; Perincek, 1990; Senel et al., 1984) and the limited geochemical data from the associated volcanic rocks are indicative for island arc formation (Yigitbas and Yilmaz, 1996). The oldest para-autochtonous cover of the Yüksekova Complex is the Late Paleocene–Eocene Seske Formation, represented mainly by neritic limestones, also found as knockers within the Kirkgecit flysch. The Kirkgecit Formation consists of olistostromal sequences with ophiolitic blocks, ranging from pebble to megablock (>1 km) sizes, which are embedded in a volcaniclastic matrix. Thick (>100 m) debris-flow conglomerates with red cherty limestone and andesite pebbles in addition to mafic and ultramafic pebbles alternate with thin layers of green-pink mudstone, pink-white pelagic limestone, beige marl and gray sandy limestone. The age of the formation as a whole, based on fossil data (Akay et al., 1989; Aksoy and Tatar, 1990; Demirtasli and Pisoni, 1965) ranges from the Middle Eocene to the Late Oligocene or possibly into the Early Miocene. The formation is intensively imbricated by relatively steep (35–40°) thrusts with south-directed vergence. To the north and northwest of Lake Van Middle and Upper Miocene is represented by Adilcevaz Limestone and Aktas conglomerates (Demirtasli and Pisoni, 1965). Both formations are involved in the end Miocene compression the following transpression tectonics. In the studied area Kirkgecit Formation is unconformably overlain by the Mehmetalan and Saray formations, respectively (Colakoglu, 2010), the former of which is also affected by thrusting and overturned folding with southerly vergence. The Pliocene–Quaternary volcanic-volcanoclastic cover is very extensive in east Anatolia.

The studied Mehmetalan, Mollatopuz and Alabayir ophiolitic units originally floating in the Kirkgecit Formation form east–west tending outcrops to the east of Lake Van (Fig. 1). The late Neogene compression and the penecontemperaneous strike-slip faults are responsible for their recent tectonic relationship with the surrounding units.

2.1. Mehmetalan and Mollatopuz ophiolites

These ophiolitic bodies form two parallel outcrops close to Mehmetalan and Mollatopuz villages, close to the Iranian border and cover a total of 15 km^2.

The Kirkgecit Formation in both areas is a proximal flysch with well-developed Bouma sequences. The lower part of the formation observed in the close vicinity of the ophiolitic body is represented by an alternation of sandstone and claystone. They gradually grade into reefal limestones. The carbonates are represented by medium-thick layered yellowish reefal limestones. Based on fossil data, the formation is Eocene in age (Acarlar et al., 1991).

In the former area, the ophiolitic body occurs as a 6 km long and 1 km wide tectonic sliver within the Kirkgecit flysch sediments (Fig. 2). The ophiolitic assemblage is disrupted by thrust-faults, marked by boudens of recrystallized neritic limestones. The dominating rock-unit of this sliver is ultramafic tectonites with rare mafic cumulates and pegmatitic gabbro. The thickness of this dismembered ophiolitic body is astimated as 500–600 m. In Mollatopuz area

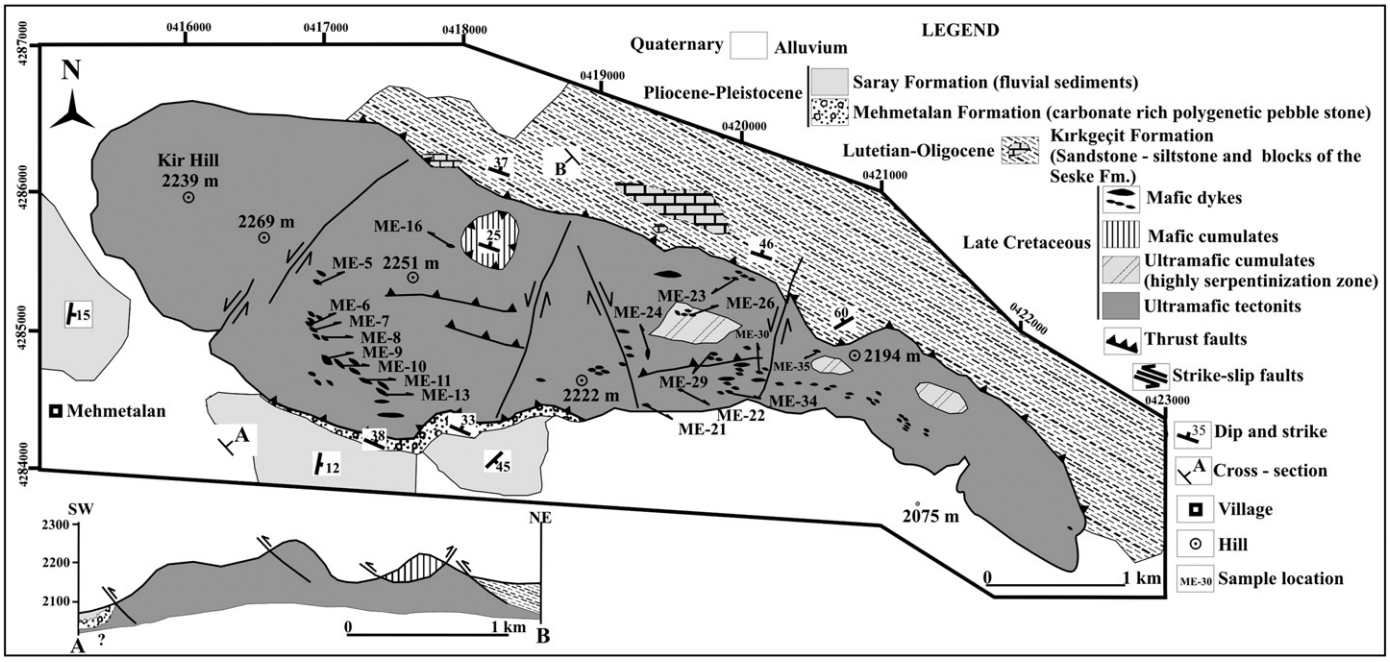

Fig. 2. Geological map and cross-section of the Mehmetalan area (modified from Colakoglu, 2010).

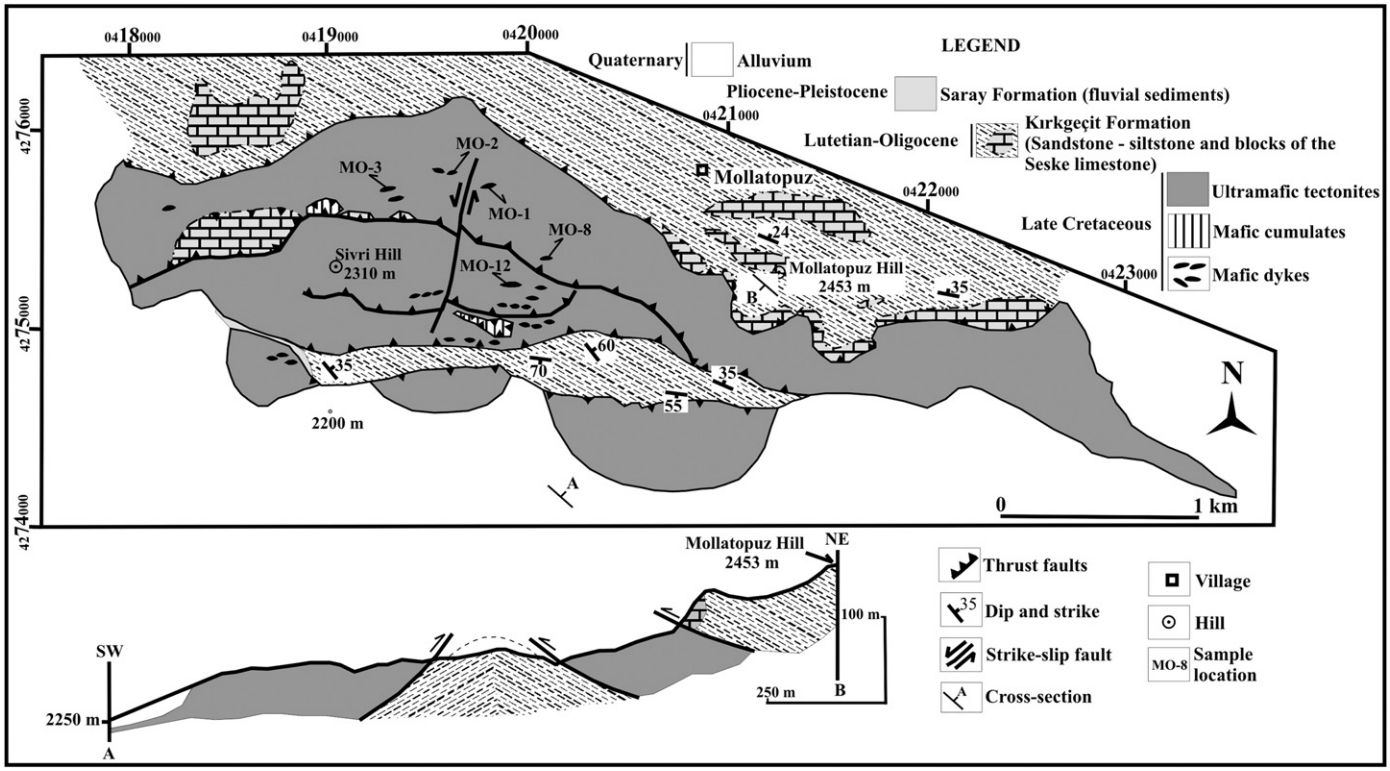

Fig. 3. Geological map and cross-section of the Mollatopuz area (modified from Colakoglu, 2010 and MTA, 2007).

(Fig. 3), the ophiolitic sliver is also more then 6 km long but more then 400 m thick. It includes next to metamorphic tectonites also ultramafic and mafic cumulates, where a ghost stratigraphy can be recognized.

In both areas the lower part of the ophiolitic body is represented by mainly by serpentinized harzburgite with subordinate dunites and pyroxenites with tectonite fabrics. The ultramafic cumulates comprise alternating dunites and pyroxenites, and the mafic cumulates are composed of normal gabbro and olivine gabbro. The ophiolite units are strongly deformed and show mylonitic texture. Dunites contain nodular, massive and banded-disseminated chromite ore and are easily distinguished by their green color in the field. These cumulates are also cut by several 5–10 cm thick pyroxenite dykes. The cumulate gabbros are seen as lenses within serpentinized harzburgite. The coarse crystalline gabbros show magmatic banding with dark and light colored mineral orientations. In general, the cumulate gabbros overlying ultramafic cumulates display regular banding, whereas those in ultramafic tectonites are pod-shaped, indicating their in-situ formation. Pegmatitic gabbros are also seen in ultramafic tectonites as boudins and dispersed blocks.

The Mehmetalan and Mollatopuz ophiolitic bodies are cut by isolated diabase dykes. The dykes are E–W oriented and boudined. Their thicknesses vary between 1 and 2 m to rarely 5 m and lengths of 4–5 to 30 m (Fig. 4a–d). These isolated diabase dykes have brown-yellowish color and partly rodingitized and shows porphyritic texture. The contact is characterized by an up to 0.6 m wide serpentinized zone.

A relatively fresh Ti-augite-phyric diabase dyke from the Mollatopuz Ophiolite (E-MORB-type sample MO-12 in Geochemistry chapter) yielded Ar/Ar plateau age of 105.4 ± 1.1 Ma, whereas another sample with SSZ-characteristics (sample ME-30 in Geochemistry chapter) from the Mehmetalan Ophiolite is dated with 92.0 ± 0.9 Ma (Günay, 2011; Günay et al., in review).

The ophiolite is covered by the Pliocene–Pleistocene Saray formation and recent alluviums. The Saray formation is composed of fluvial pebblestones and coarse grained sandstones, dominated by ophiolitic and volcanic clasts.

2.2. Alabayir ophiolite

The Alabayir ophiolite, the westernmost of the studied ophiolitic bodies, differs from the others in regard to its geological setting and the geochemical properties of the mafic dykes. This ophiolitic body occurs as a tectonic slice with tectonic contacts both to the Upper Paleocene–Eocene fossiliferuos limestones (Toprakkale Formation in Acarlar et al., 1991) in the Kirkgecit flysch and the Upper Oligocene–Early Miocene Van formations (Fig. 5). The latter is made up of sandstone and shale alternations and represents the upper part of the Kirkgecit Formation.

The Alabayir ophiolite body is elliptical in shape and represented by serpentinized harzburgite, serpentinite, dunite, pyroxenite dykes and chromite ore. The partly preserved mafic cumulate units consist of olivine gabbro, troctolite and layered gabbro. Ribbons of recrystallized limestone within the ophiolite mark the thrust planes, otherwise not recognizable in the serpentinized body.

The ultramafic and mafic units of Alabayir ophiolite are cut by isolated diabase dykes. Diabase dykes extend in NE–SW direction and are 2–4 m thick and 30–40 m long. The dykes are consistent with the general trend of the ophiolitic body. Diabase dykes are blackish in color and plagioclase-phryic.

Preliminary Ar/Ar whole rock dating of one sample (C-4) from the Alabayir dyke yielded a plateau age of 87.7 ± 1.0 Ma (Günay, 2011; Günay et al., in review).

3. Petrography of mafic dykes

The petrographic properties of mafic dykes in Mehmetalan–Mollatopuz and Alabayir ophiolitic bodies show differences (Fig. 6a–d). Isolated diabase dykes in Mehmetalan and Mollatopuz ophiolites are partly rodingitized. These mafic dykes always show ophitic texture.

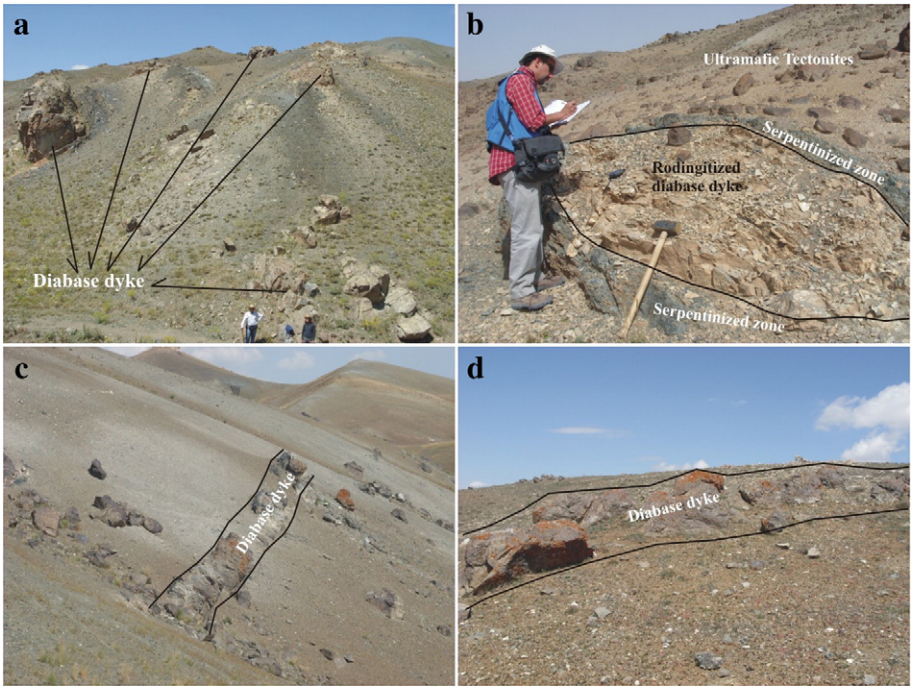

Fig. 4. Field photographs showing (a–b) general view of diabase dykes from Mehmetalan (c). E–W trending diabase dyke within serpentinite in the Mollatopuz area (d) diabase dyke within the Alabayir ophiolite.

The igneous mineral paragenesis is plagioclase, clinopyroxene, phlogopite, orthopyroxene and opaque minerals, whereas hydrogrossular (hibshite), chlorite, actinolite, epidote, apatite and calcite occur as secondary minerals. Rarely, some unaltered dolerite dykes are also found (e.g. sample MO-12 on Fig. 5b). The anhedral pyroxenes are diopsitic–augitic in composition. Uralitization and chloritization are common in pyroxene. The observed hibshites are the most frequent metasomatic products in the dykes (Fig. 6a, d). Apatite and opaque minerals are found as accessories. The assemblage of calcite, titanite, actinolite, chlorite and epidote confirms that the mafic dykes have been subjected to low-grade metamorphism (Elthon, 1979; Spear, 1981).

The isolated diabase dykes in the Alabayir ophiolite consist of green and brown hornblende, plagioclase, biotite, clinopyroxene, chromite and opaque minerals as primary igneous phases. Chlorite, epidote, apatite, calcite and quartz are secondary minerals (Fig. 5c,

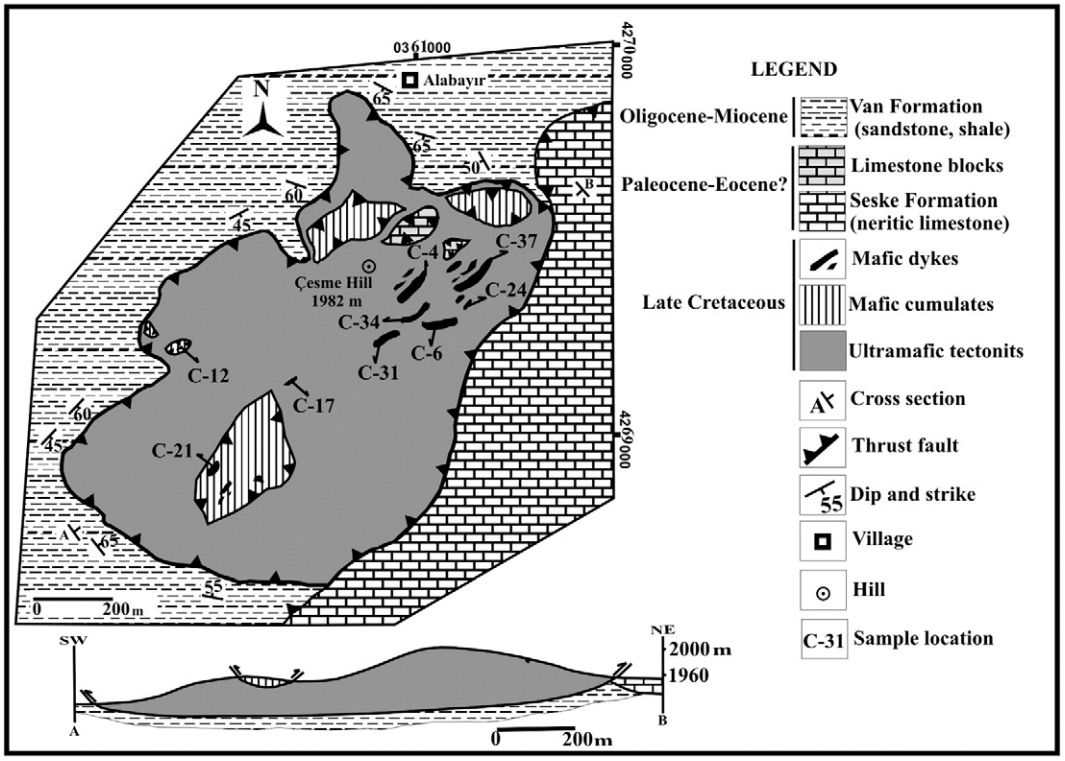

Fig. 5. Geological map and cross-section of the Alabayir area (modified from Colakoglu, 2010).

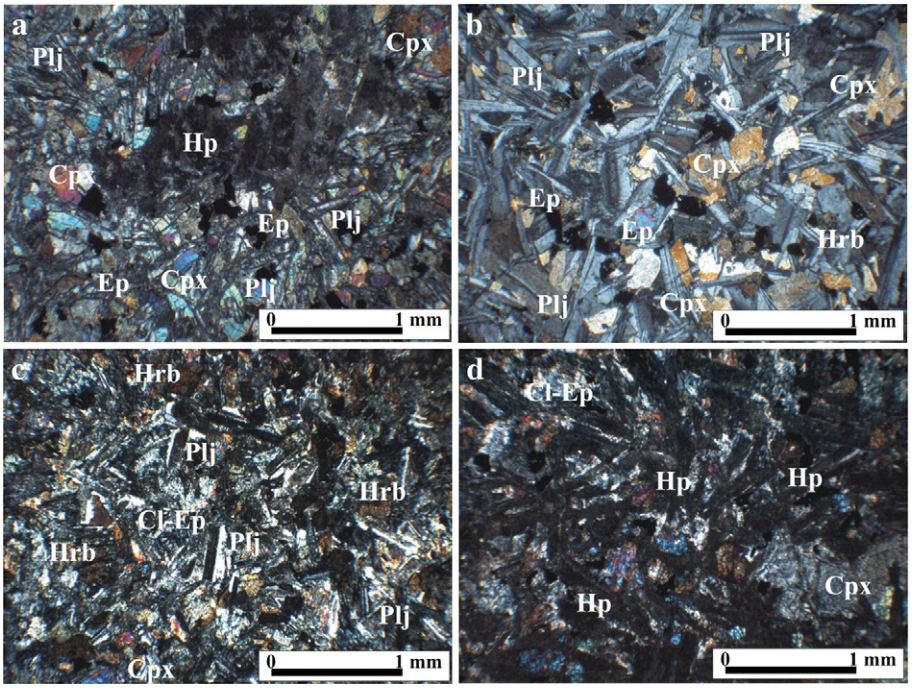

Fig. 6. Microphotographs of diabase dykes in the study area (a) mineral assemblage (hibshite, plagioclase, clinopyroxene and epidote) and texture from the Mehmetalan diabase dyke (sample ME-13), (b) ophitic texture of unaltered diabase dyke (sample no MO-12), (c) altered diabase dyke with subophitic texture (sample C-4), (d) rodingitized diabase dyke from Mehmetalan (sample C-4). Abbreviations: hibshite (Hp), hornblend (Hrb), plagioclase (Plj), chlorite (Cl), epidote (Ep), clinopyroxene (Cpx).

d). They exhibit ophitic and sub-ophitic texture. Plagioclases are found both as phenocrysts and fine-grained prismatic crystals. Amphiboles are observed as both primary hornblende and secondary actinolite. Both green and brown hornblendes are found as small anhedral crystals. The biotites are pleochroic brown and anhedral in shape. Clinopyroxenes are generally diopsitic and Ti-augitic in composition and show partly uralitization. The sericitization in plagioclase, chloritization and epidotization in amphiboles are observed as alteration products. Apatite and zircon are found as accessory minerals. All chromites are separated from other opaques by their light brown color. The diabase dykes in contact with chromite ore contain chromite crystals.

4. Geochemistry

4.1. Analytical methods

Thirty two samples collected from the study area were analyzed for major, trace and Rare Earth Elements (REE) in ALS Chemex Laboratory (Canada). Major oxides were analyzed by X-ray fluorescence spectrometry. Ignited sample (0.9 g) is added to 9.0 g of Lithium Borate Flux (50%–50% Li_2 B_4O_7–$LiBO_2$), mixed well and fused in an auto fluxer between 1050 and 1100 °C. Trace elements and REE were analyzed by Inductively Coupled Plasma-Mass Spectroscopy (ICP-MS). A prepared sample (0.200 g) is added to lithium metaborate flux (0.90 g), mixed well and fused in a furnace at 1000 °C. The resulting melt is then cooled and dissolved in 100 mL of 4% HNO_3/2% HCl solution. This solution is then analyzed by inductively coupled plasma-mass spectrometry. Quality control limits for reference materials and duplicate analyses are established according to the precision and accuracy requirements of the particular method. The results are reported in Table 1.

4.2. Element mobility

Highly variable loss on ignition (LOI) values displayed by mafic dykes (1.2–7.0 wt.%) are indicative of low-grade hydrothermal alteration, as also confirmed by petrographic observations, which may lead to selective element mobility. Thus, we consider mainly of HFSE and REE in our petrogenetic interpretations, which are known as relatively immobile under conditions of low-grade alteration/metamorphism (e.g. Pearce and Cann, 1973). When plotted against Zr (a fluid-immobile element), elements of low-ionic potential (e.g. Ba, K, Rb except Th) show scattered distribution, whereas high-field strength elements (HFSE) and REE display well-defined trends, (Fig. 7) showing their stable nature.

The existence of chlorite, hibshite and diopside in mafic dykes of Mehmetalan and Mollatopuz ophiolites as indicative of an earlier stage of rodingitization (Tsikouras et al., 2009) is characterized by introduction of calcium and removal of alkalies (Austrheim and Prestvik, 2008; Coleman, 1967). The presence of hydrogrossular is consistent with a fluid character in which the silica activity was low. This fluid may have been derived from the serpentinization processes (e.g. Frost and Beard, 2007), which is also consistent with major oxide data obtained from rodingitized mafic dykes in the Mehmetalan and Mollatopuz ophiolites.

4.3. Results

The studied sample suites span a large range in terms MgO and Ni, indicating that they have experienced fractional crystallization, and the relatively low values suggest that they do not represent mantle-derived primary magma compositions (e.g. Hart and Davis, 1978). On the basis of Zr/TiO_2 versus Nb/Y plot (Winchester and Floyd, 1977), the Mehmetalan and Mollatopuz dykes have subalkaline composition, whereas Alabayir dykes display alkaline character (Fig. 8a). This compositional difference between the suites is further supported by the tholeiitic nature of the Mehmetalan and Mollatopuz suites; they have lower P_2O_5 at a given Zr, when compared with Alabayir (Fig. 8b, Floyd and Winchester, 1975).

Multi-element patterns normalized to normal-MORB (N-MORB) reveals that the Mehmetalan and Mollatopuz samples show similar geochemical characteristics, whereas the Alabayir samples appear to be quite different. All Mehmetalan and Mollatopuz dykes (with

Table 1
Major and trace element data for the Mehmetalan (ME), Mollatopuz (MO), and Alabayir (C) diabase dykes.

		ME-5	ME-6	ME-7	ME-8	ME-9	ME-10	ME-11	ME-13	ME-16	ME-21	ME-22	ME-23	ME-24	ME-26	ME-29	ME-34
D.L. %		Major oxide %															
SiO_2	0.01	42.70	43.80	42.10	43.70	44.60	43.10	44.80	38.20	43.10	43.10	41.50	39.00	42.40	42.50	47.10	38.10
Al_2O_3	0.01	14.15	14.95	13.75	14.85	14.60	15.15	14.80	12.75	14.55	14.70	14.85	14.75	14.65	17.65	15.05	11.45
Fe_2O_3	0.01	10.40	9.96	10.80	10.05	10.55	10.05	10.70	9.01	9.43	10.95	10.10	9.18	10.10	8.09	11.80	11.30
CaO	0.01	10.05	10.75	13.65	11.35	10.80	10.50	10.95	19.30	10.40	9.68	10.65	20.20	10.75	15.05	10.20	25.70
MgO	0.01	7.14	7.01	6.58	6.74	6.61	6.70	6.65	9.03	7.59	6.90	5.86	8.50	5.79	8.36	6.98	4.93
Na_2O	0.01	6.76	6.04	5.38	5.30	4.90	6.06	5.32	3.10	5.75	6.06	7.75	1.89	7.06	2.56	3.78	2.02
K_2O	0.01	0.65	0.56	0.21	0.47	0.74	0.44	0.61	0.01	1.95	0.84	0.56	0.02	1.18	0.18	0.45	0.03
Cr_2O_3	0.01	0.04	0.03	0.03	0.03	0.03	0.03	0.03	0.06	0.05	0.04	0.04	0.05	0.03	0.05	0.03	0.01
TiO_2	0.01	1.18	1.11	1.26	1.10	1.20	1.13	1.22	0.87	0.99	1.28	1.29	0.91	1.24	0.75	1.41	1.57
MnO	0.01	0.18	0.17	0.18	0.17	0.18	0.17	0.18	0.15	0.16	0.19	0.17	0.16	0.17	0.14	0.20	0.19
P_2O_5	0.01	0.12	0.10	0.13	0.09	0.11	0.11	0.13	0.07	0.10	0.12	0.11	0.09	0.12	0.07	0.14	0.19
LOI		6.41	5.46	5.56	4.95	3.87	5.20	4.23	6.34	5.41	5.07	6.95	5.51	6.73	4.25	2.50	4.63
Total		99.80	100	99.80	98.90	98.20	98.70	99.70	98.90	99.50	99.00	99.90	100.5	100	99.8	99.8	100
D.L. ppm		Trace element ppm															
Cr	10	240	230	180	210	210	230	220	420	330	280	310	370	210	350	190	60
Ba	0.5	14	70.80	216	139	102	52	231	20.80	53.70	174	17.50	27.60	14	747	689	13.60
Rb	0.2	38	28.90	14.80	25	29	18.70	31.60	1.20	118	42.30	31.10	1.50	50.50	3.60	9.40	1.40
Sr	0.1	112	240	842	253	334	194.5	292	204	65.9	353	154	181	113	579	424	71
Th	0.05	0.63	0.53	0.74	0.56	0.69	0.60	0.69	0.40	0.53	0.52	0.50	0.43	0.55	0.39	0.88	1.53
Nb	0.2	3.80	3.40	4.20	3.40	3.90	3.60	4.10	2.60	4.00	3.60	3.60	2.70	3.60	2.20	4.80	11.80
Ta	0.1	0.20	0.20	0.20	0.20	0.20	0.20	0.20	b.d.	0.20	0.20	0.20	0.20	0.20	0.10	0.30	0.70
Zr	2	78	73	87	75	82	77	92	57	65	86	81	59	84	48	97	116
Y	0.5	27.20	25.80	29.50	26.00	28.80	26.90	29.80	20.90	23.00	30.00	28.20	21.80	29.40	17.90	32.80	32.40
V	5	248	244	267	240	259	245	267	205	226	275	268	210	261	176	306	295
Hf	0.2	2.20	2.10	2.40	2.20	2.30	2.10	2.50	1.60	1.80	2.40	2.30	1.70	2.40	1.40	2.70	3.20
Ga	0.1	12.60	15.10	13.10	15.60	16.10	12.40	17.00	9.50	13.40	13.20	12.40	11.90	13.80	14.00	17.90	14.30
U	0.05	0.13	0.10	0.15	0.11	0.14	0.12	0.14	0.08	0.10	0.11	0.11	0.09	0.12	0.07	0.18	0.36
D.L. ppm		Rare earth element ppm															
La	0.5	6.20	5.30	6.70	5.40	6.70	5.90	6.70	4.30	5.30	5.60	5.30	4.40	5.50	4.50	7.70	12.90
Ce	0.5	14.70	13.00	16.00	13.50	15.30	14.10	15.70	10.40	12.70	14.00	13.10	10.80	13.70	10.40	18.40	28.10
Pr	0.03	2.06	1.84	2.28	1.87	2.09	1.95	2.20	1.46	1.77	2.04	1.88	1.51	1.96	1.37	2.56	3.65
Nd	0.1	10.10	9.00	11.00	9.20	10.20	9.80	10.70	7.20	8.60	10.10	9.50	7.60	9.80	7.00	12.50	16.10
Sm	0.03	3.12	3.00	3.37	2.93	3.13	3.08	3.24	2.33	2.61	3.24	3.03	2.42	3.13	2.08	3.78	4.41
Eu	0.03	1.20	1.12	1.27	1.19	1.27	1.21	1.29	0.95	1.01	1.27	1.23	0.95	1.27	0.85	1.47	1.63
Gd	0.05	3.71	3.40	4.22	3.50	3.88	3.53	4.03	2.85	3.14	3.95	3.74	2.92	3.93	2.56	4.51	4.99
Tb	0.01	0.71	0.65	0.77	0.66	0.74	0.66	0.74	0.52	0.57	0.76	0.72	0.54	0.73	0.47	0.85	0.87
Dy	0.05	4.58	4.27	4.97	4.31	4.88	4.48	4.80	3.46	3.75	4.96	4.71	3.64	4.93	3.01	5.46	5.57
Ho	0.01	1.02	0.94	1.10	0.96	1.07	1.00	1.06	0.77	0.84	1.10	1.05	0.83	1.07	0.65	1.23	1.20
Er	0.03	3.13	2.89	3.45	2.92	3.20	2.97	3.30	2.28	2.58	3.38	3.16	2.43	3.33	2.01	3.71	3.71
Tm	0.01	0.44	0.42	0.48	0.40	0.46	0.42	0.47	0.34	0.37	0.49	0.46	0.37	0.49	0.29	0.55	0.53
Yb	0.03	2.84	2.73	3.09	2.69	2.93	2.73	3.04	2.22	2.39	3.12	2.98	2.28	3.04	1.86	3.55	3.34
Lu	0.01	0.44	0.41	0.48	0.42	0.46	0.43	0.48	0.33	0.37	0.50	0.45	0.36	0.46	0.29	0.54	0.52

		ME-35	ME-30	MO-1	MO-2	MO-3	MO-8	MO-12	C-4	C-6	C-12	C-17	C-21	C-24	C-31	C-34	C-37
D.L. %		Major oxide %															
SiO_2	0.01	43.10	47.10	37.90	39.10	41.80	49.60	46.90	50.70	51.00	52.40	47.50	52.70	47.00	43.30	52.20	42.80
Al_2O_3	0.01	15.25	15.55	13.70	13.10	13.25	14.55	14.95	14.90	16.60	17.35	14.65	15.65	16.35	14.95	15.00	15.35
Fe_2O_3	0.01	9.25	11.05	8.95	9.53	9.70	10.80	11.90	10.75	8.26	8.25	10.35	9.81	7.74	9.07	8.78	8.84
CaO	0.01	14.55	11.35	24.80	23.20	20.40	11.60	12.40	8.54	9.28	8.18	14.45	7.40	16.80	19.05	9.32	18.65
MgO	0.01	9.13	7.21	6.19	6.43	6.20	5.34	6.82	4.75	4.04	4.06	3.45	4.20	4.23	5.53	4.68	6.11
Na_2O	0.01	2.63	2.86	1.62	1.74	2.04	2.85	2.51	4.78	3.76	4.19	3.19	4.57	2.26	0.91	4.30	0.36
K_2O	0.01	0.29	0.86	0.02	0.04	0.10	0.93	0.31	0.78	1.52	1.63	1.72	1.65	0.90	0.92	0.87	0.23
Cr_2O_3	0.01	0.06	0.03	0.03	0.03	0.03	0.01	0.03	0.39	0.11	0.03	0.02	0.02	0.02	0.03	0.02	0.04
TiO_2	0.01	0.90	1.24	1.03	1.12	1.16	0.59	1.70	1.76	1.28	1.28	1.76	1.73	1.24	1.53	1.42	1.49
MnO	0.01	0.16	0.19	0.15	0.16	0.17	0.16	0.20	0.17	0.14	0.15	0.17	0.17	0.14	0.16	0.15	0.15
P_2O_5	0.01	0.09	0.13	0.09	0.11	0.10	0.04	0.20	0.50	0.45	0.44	0.54	0.46	0.32	0.41	0.36	0.39
LOI		4.66	2.48	5.52	5.53	4.86	3.46	1.90	1.18	2.08	1.57	2.25	1.28	2.17	4.33	2.58	4.83
Total		100.5	100	100	100	100	100.5	99.90	99.30	98.70	99.70	100.5	99.90	99.20	100	99.80	99.30
D.L. ppm		Trace element ppm															
Cr	10	400	190	210	220	200	70	210	1740	630	170	110	150	150	150	110	220
Ba	0.5	1135	325	16.70	31.40	66.10	70	66.20	192.5	760	655	2000	1325	311	158.5	641	42.1
Rb	0.2	6.90	18	0.50	1.60	2.70	11.60	7.50	10.90	28.40	28.70	31.20	24.60	16.70	17.70	14.50	2.20
Sr	0.1	520	628	143	614	2610	270	248	275	487	810	607	651	269	131.5	303	76.80
Th	0.05	0.43	0.65	0.47	0.50	0.54	0.32	0.89	4.33	6.32	6.13	6.17	6.81	4.56	5.58	5.42	5.60
Nb	0.2	2.70	3.70	3.20	3.50	3.70	1.90	9.90	47.80	55.80	53.60	48.30	53.00	46.10	45.20	50.60	46.20
Ta	0.1	b.d.	0.20	0.20	0.20	0.20	b.d.	0.60	2.90	3.00	2.90	2.50	3.10	2.50	2.50	2.70	2.60
Zr	2	59	83	65	71	74	29	119	183	178	169	189	206	164	182	183	190
Y	0.5	21.90	29.10	23.70	25.30	26.80	17.60	28.80	28.60	26.90	26.30	32.30	28.90	23.60	26.40	28.50	26.70
V	5	213	269	229	245	252	312	264	199	170	174	210	203	143	175	165	174
Hf	0.2	1.70	2.40	1.90	2.00	2.20	1.00	3.20	3.70	3.50	3.40	3.70	4.20	3.20	3.60	3.70	3.70

(continued on next page)

Table 1 (*continued*)

		ME-35	ME-30	MO-1	MO-2	MO-3	MO-8	MO-12	C-4	C-6	C-12	C-17	C-21	C-24	C-31	C-34	C-37
D.L. ppm		Trace element ppm															
Ga	0.1	13.80	16.90	10.30	9.40	11.50	14.30	18	16.80	16.80	18	17.10	19.30	15	15.60	16.20	15.40
U	0.05	0.08	0.13	0.10	0.10	0.11	0.09	0.21	1.16	1.61	1.62	1.65	1.69	1.19	1.40	1.39	1.41
D.L. ppm		Rare earth element ppm															
La	0.5	4.60	6.20	4.80	5.20	5.40	2.60	9.70	42.10	52.50	51.20	50.70	48.70	36.90	41.50	44.50	41.70
Ce	0.5	11.00	15.10	11.70	12.60	13.30	5.70	23.10	79.80	94.10	91.20	90.50	86.40	67	75.80	79.70	75
Pr	0.03	1.53	2.10	1.63	1.74	1.84	0.75	3.11	9.32	10.40	9.87	9.92	9.45	7.43	8.36	8.85	8.39
Nd	0.1	7.80	10.60	8.20	8.70	9.30	4	14.40	33.90	36.50	35.50	35.50	34	26.90	31.10	31.60	30.80
Sm	0.03	2.39	3.32	2.73	2.75	2.96	1.33	4.05	6.30	6.79	6.41	6.84	6.56	5.01	5.96	6.15	5.93
Eu	0.03	1.01	1.30	1.09	1.07	1.15	0.56	1.54	2.04	1.93	1.87	1.95	1.97	1.53	1.81	1.84	1.77
Gd	0.05	3.00	3.99	3.17	3.37	3.59	1.87	4.63	6.65	6.61	6.43	6.94	6.64	5.11	6.20	6.29	6.03
Tb	0.01	0.55	0.72	0.60	0.62	0.67	0.39	0.81	0.95	0.89	0.85	0.97	0.89	0.74	0.85	0.87	0.83
Dy	0.05	3.63	4.85	3.95	4.12	4.41	2.73	4.99	5.48	4.97	4.84	5.77	5.37	4.21	4.91	5.14	4.83
Ho	0.01	0.82	1.07	0.88	0.94	0.98	0.63	1.05	1.10	1.00	0.97	1.17	1.07	0.86	1.00	1.05	1.00
Er	0.03	2.42	3.29	2.70	2.80	3.00	2.01	3.20	3.11	2.91	2.87	3.52	3.13	2.53	2.90	3.18	2.90
Tm	0.01	0.35	0.47	0.37	0.42	0.42	0.31	0.44	0.49	0.40	0.42	0.50	0.45	0.36	0.41	0.44	0.41
Yb	0.03	2.33	2.98	2.51	2.66	2.79	2.09	2.88	2.67	2.55	2.51	2.99	2.80	2.26	2.55	2.65	2.51
Lu	0.01	0.36	0.47	0.37	0.42	0.44	0.31	0.44	0.40	0.37	0.37	0.45	0.41	0.35	0.39	0.41	0.38

Explanation: LOI: loss of ignition; Fe_2O_3 is given as total Fe (b.d.: below detections limits; D.L.: Detection Limit).

some exceptions as explained below) display variable enrichment in Th, coupled with N-MORB-like HFSE distribution (Fig. 9a, will be called Type-1; Th/Nb = 0.13–0.18), and they are akin to SSZ-type basalts (e.g. Pearce et al., 1984). Within Type-1 group, MO-8 appears to be different relative to the rest. This sample not only has the most depleted chemistry within the group, but it also shows some diversity in terms of trace element systematics. It has a different nature with relative depletion of HFSE compared to Y and HREE. Among Mehmetalan and Mollatopuz samples, ME-34 and MO-12 are distinct relative to Type-1 in that they are apparently of more enriched nature, somewhat resembling E-MORB-type basalts (Fig. 9b, will be called Type-2; e.g. Sayit et al., 2010; Sun and McDonough, 1989). It must be noted, however, that ME-34 is still slightly enriched in Th relative to Nb and Ta (Th/Nb = 0.13), whereas this feature is not observed in MO-12 (Th/Nb = 0.09). The Alabayir dykes are markedly different than the Mehmetalan and Mollatopuz dykes, and show apparent enrichment in immobile incompatible trace elements, being more akin to oceanic island-type basalts (OIB) (Fig. 9c, e.g. Chauvel et al., 1992; Workman et al., 2004).

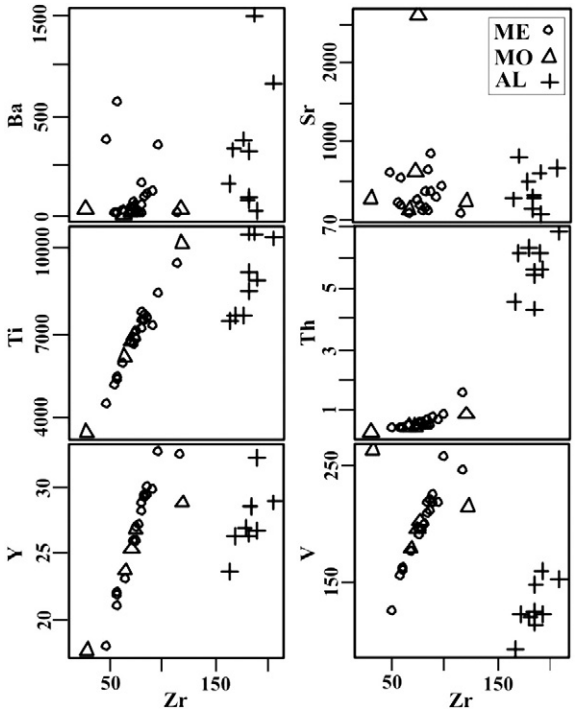

Fig. 7. Variation of selective trace elements against 24 Zr, suggesting that LIL elements (except Th) have been mobilized by post-magmatic processes, whereas HFSE have remained relatively undisturbed.

Type-1 Mehmetalan and Mollatopuz samples are characterized by nearly flat chondrite-normalized REE patterns (except MO-8), with LREE being slightly enriched relative to HREE (Fig. 10a, $[Ce/Yb]_N = 1.22–1.48$; normalization values from Sun and McDonough (1989)). MO-8 is differentiated from the rest of Type-1 samples in displaying marked LREE depletion over HREE ($[Ce/Yb]_N = 0.76$). Type-2 samples ME-34 and MO-12 are dissimilar relative to Type-1, with HREE fractionated over LREE (Fig. 10b, $[Ce/Yb]_N = 2.23–2.34$). Dark grey fields shown in Fig. 10 a,b. compiled from Ewart et al., 1994 a,b; Dupuis et al., 2005. The Alabayir dykes, on the other hand, have the most fractionated patterns among the studied samples, displaying strong depletion of HREE over LREE (Fig. 10c, $[Ce/Yb]_N = 8.24–10.25$).

4.4. Petrogenesis

The depleted-type Mehmetalan and Mollotopuz dykes (Type-1) are characterized by high Zr/Nb (15.3–23.9), Y/Nb (5.8–9.3), and low Zr/Y (1.7–3.1) ratios, suggesting that a depleted mantle source (N-MORB source) has been involved in their petrogenesis. This idea is further supported by N-MORB-like or depleted HFSE abundances relative to N-MORB. In the latter case (i.e. MO-8), it further indicates a source region that may have experienced a previous melt extraction (e.g. Woodhead et al., 1993). In contrast to Type-1 dykes, lower Zr/Nb, Y/Nb, and higher Zr/Y ratios of the enriched-type (Type-2) Mehmetalan and Mollotopuz dykes (9.8–12.0; 2.8–2.9; 3.6–4.1, respectively) and Alabayir suite (3.2–4.1; 0.5–0.7; 5.9–7.1, respectively) can be attributed to a more enriched source region and/or generation under smaller degrees of partial melting. This relative difference in enrichment between the studied suites is also reflected by the absolute abundances of Zr and Nb which are lowest in Type-1 Mehmetalan and Mollotopuz samples, and highest in the Alabayir samples.

A characteristic feature of the Type-1 Mehmetalan and Mollatopuz dykes is the relative enrichment of Th over HFSE. Negative Nb anomalies (high Th/Nb) ratios coupled with relatively depleted HFSE patterns (with respect to N-MORB) are typical of supra-subduction zone- (SSZ) type basalts from intra-oceanic environments (e.g.

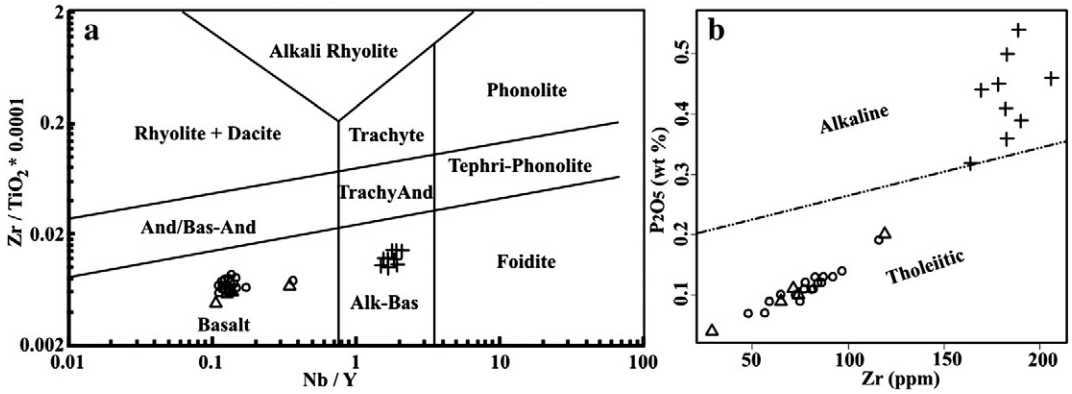

Fig. 8. a–b. Chemical discrimination of the Mehmetalan, Mollatopuz, and Alabayir diabase dykes on the basis of immobile elements (after Winchester and Floyd, 1977).

Pearce et al., 1995a; Sinton et al., 2003). The lower Ti/V ratios of the Type-1 suite (11.3–28.9) compared to Type-2 (31.9–38.6) and the Alabayir suites (44.1–53.0) further confirms their derivation from a more depleted source region, since low Ti/V ratios are commonly associated from basalts from MORs and supra-subduction zones (Fig. 11a) (e.g. Shervais, 1982). It is noteworthy to mention that MO-8 has the lowest Ti/V value as expected from its highly depleted character. E-MORB-like Type-2 samples seems to be in between Type-1 and Alabayir samples, which is in good agreement with the previous results.

Nb/Yb–Th/Yb plot is very effective in monitoring contributions from within-plate processes and subduction-related events (Pearce

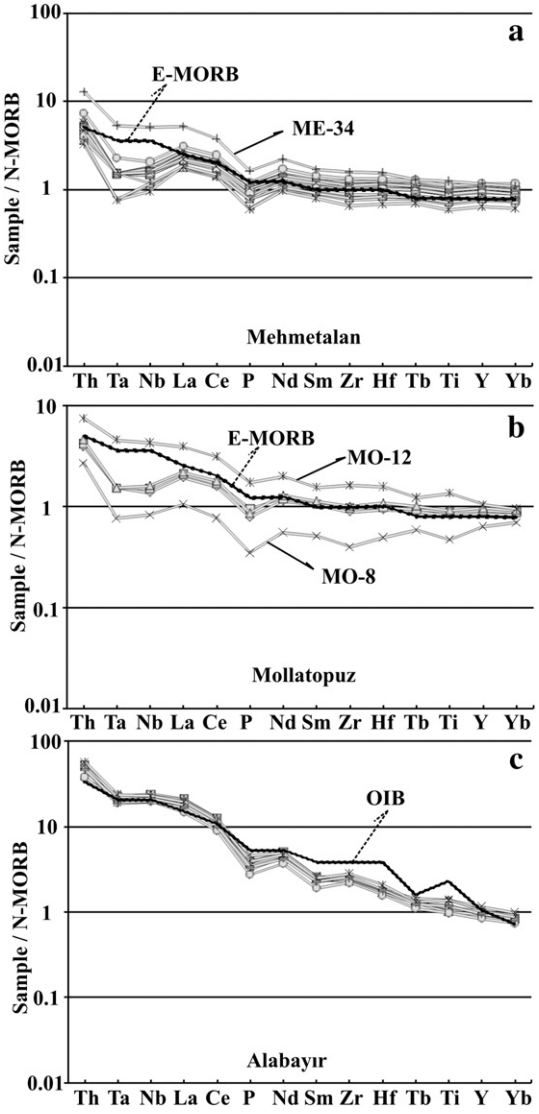

Fig. 9. N-MORB-normalized trace element patterns of the dyke samples (normalization values from Sun and McDonough, 1989).

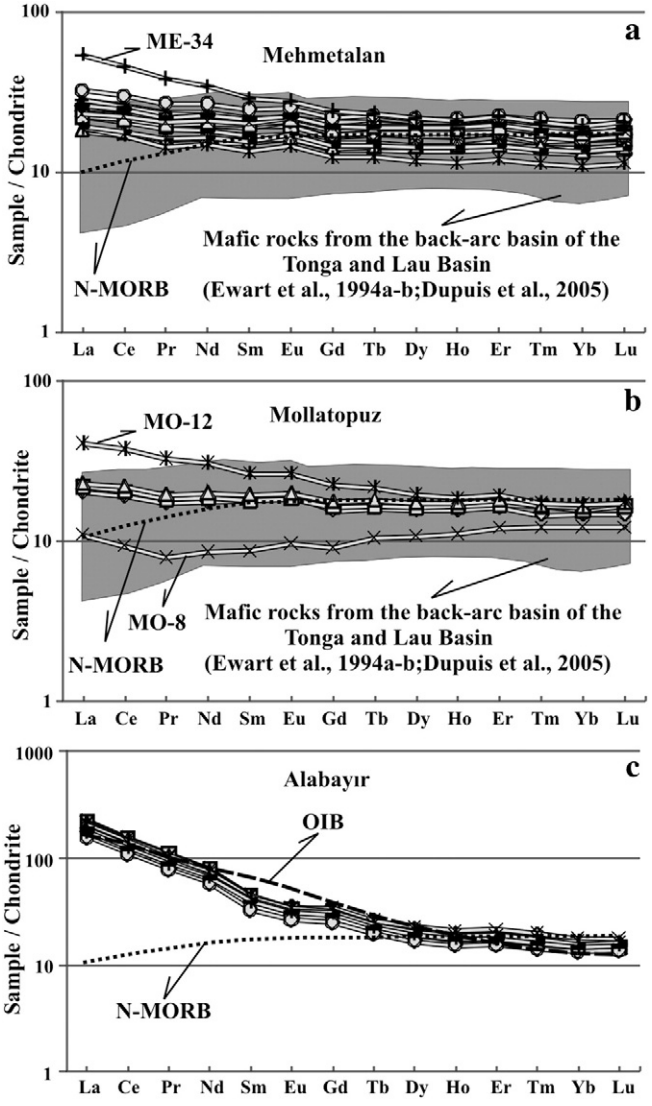

Fig. 10. Chondrite-normalized REE patterns of the dyke suites (normalization values from Sun and McDonough, 1989).

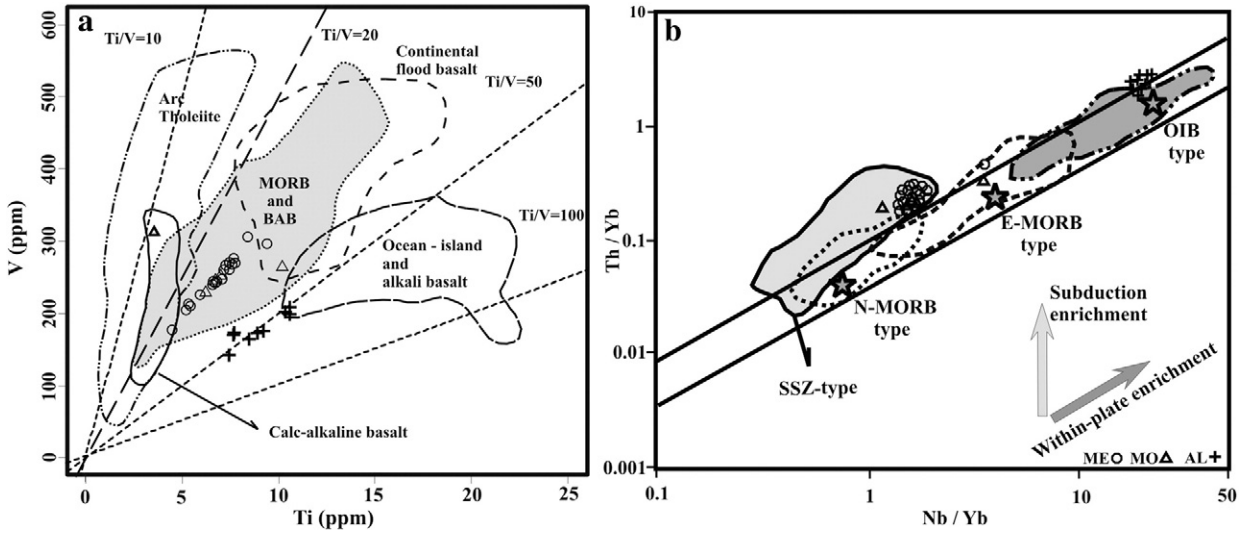

Fig. 11. Variations of a) Ti–V (after Shervais, 1982) and b) Th/Yb–Nb/Yb systematics of the studied samples (after Pearce and Peate, 1995). Average N-MORB, E-MORB and OIB compositions from Sun and McDonough (1989). SSZ-, N-MORB-, E-MORB-, and OIB-type fields compiled from Maheo et al. (2004), Saccani and Photiades (2005), Aldanmaz et al. (2008), and Göncüoglu et al. 2010. The Göksun sheeted dyke is from Parlak et al. (2004).

and Peate, 1995). In this plot, basalts generated from a mantle source with no subduction influence would be aligned in a linear manner, since Th and Yb become equally enriched during within-plate processes. Any influence from subduction-related processes, however, will cause Th to be displaced towards higher values relative to Nb, thus leading to higher Th/Yb values at a given Nb/Yb (Pearce, 1983). In this plot, it is seen that the Alabayir dykes display strong within-plate enrichment as can be expected from their OIB-like nature. It is revealed that all Mehmetalan and Mollatopuz samples except for Type-2 MO-12 have been variably affected by the subduction component (Fig. 11b). Taken into account the low Nb/Yb ratios of the Type-1 suite, this indicates a depleted source region that has been fluxed by subduction-related processes for their genesis. This result further confirms the intra-oceanic SSZ-character of these samples. Type-2 sample MO-12 and the Alabayir samples, however, appear to have been least modified by this component; only some of them have slightly higher Th/Yb ratios (Fig. 11b).

4.5. Melting model

In order to put further constraints on nature of the source region and degree of melting, we apply two separate modelling schemes. This is due to the fact the studied suites comprise both depleted (N-MORB-type, Type-1 suite) and enriched (E-MORB- and OIB-type, Type-2 and Alabayir) samples. We must note, however, that melt models are based on selection of the partition coefficients and the source/melt modes, so our aim here is to bring some approximation regarding the melting processes. Regarding the depleted samples, we use a geochemical modelling on the basis of Nb–Y systematics devised by Pearce and Parkinson (1993) (for the details of this melting model, the reader is referred to their study). To perform this, we corrected the samples (with MgO > 7%) for fractionation back to 9% MgO, using least-squares linear regression. The modelling suggest that ca. 10%–30% partial melting of a fertile spinel-lherzolite source can explain the observed composition of Type-1 samples (Fig. 12a). The sample MO-8, however, is relatively evolved (with 5.3% MgO wt.%), we could not apply the Nb–Y systematics on this sample. However, on the Cr–Y plot of Murton (1989), although it is difficult to make an estimation about the degree of melting due to the uncertainty about its fractionation path, we can at least say that this sample requires an already depleted source (not shown).

To model the enriched-type samples, we use a melting systematics on the basis of LREE/MREE and MREE/HREE ratios. In this way, we can monitor better the effect of residual garnet, which can strongly fractionate HREE over LREE and MREE. We also assume that any LREE–MREE fractionation that can be caused by addition of subduction components is negligible. Although the Alabayir suite are somewhat evolved (MgO ~3.5–6.1 wt.%) compared to those from other suites, the plots of Mg# (or MgO) vs Ce/Sm and Sm/Yb display no meaningful relationship (not shown), therefore we believe that the observed ratios mainly reflect variations related to partial melting and/or source processes rather than fractional crystallization. The plot suggests that the Alabayir samples can be modelled by about 1–2% partial melting of a garnet–lherzolite source with primitive mantle (PM) composition (Fig. 12b). Type-2 samples requires a different melting scheme as expected, and they reflect 6–7% melting of a similar garnet lherzolite source. The melting systematics of Type-2 samples can also be explained by melting of a mixed PM-DM source, or alternatively of a mantle source with DM composition (not shown). However, in all cases, the source appears to contain some amount of residual garnet.

5. Discussion

Geochemical examination of the studied ophiolitic suites reveals three different compositional groups. The first of these is SSZ-type basalts, characterized by largely N-MORB-like HFSE distribution coupled with a subduction component (elevated Th/Nb). Type-1 Mehmetalan and Mollatopuz samples are representative of this group. The second group includes E-MORB-type basalts with overall enrichment of immobile incompatible elements relative to N-MORB, and covers Type-2 samples (ME-34 and MO-12). ME-34, however, differ from MO-12 by having a higher Th/Nb ratio, thus reflecting a subduction-derived component in its source region. The last group, represented by the Alabayir dykes, is characterized by OIB-type signatures with marked enrichment in incompatible elements with respect to N-MORB.

Type-1 Mehmetalan and Mollatopuz dykes have trace element ratios indicative of derivation from a subduction-modified depleted mantle. Such features (e.g. high LILE/HFSE, LREE/HFSE) is typical in SSZ-type basalts and have been attributed to refertilization of mantle wedge by slab-derived fluids/melts (e.g. Arculus and Powell, 1986; Class et al., 2000; Elliott et al., 1997; Pearce and Peate, 1995). The transitional nature between MORB and IAT (Fig. 13), and relatively

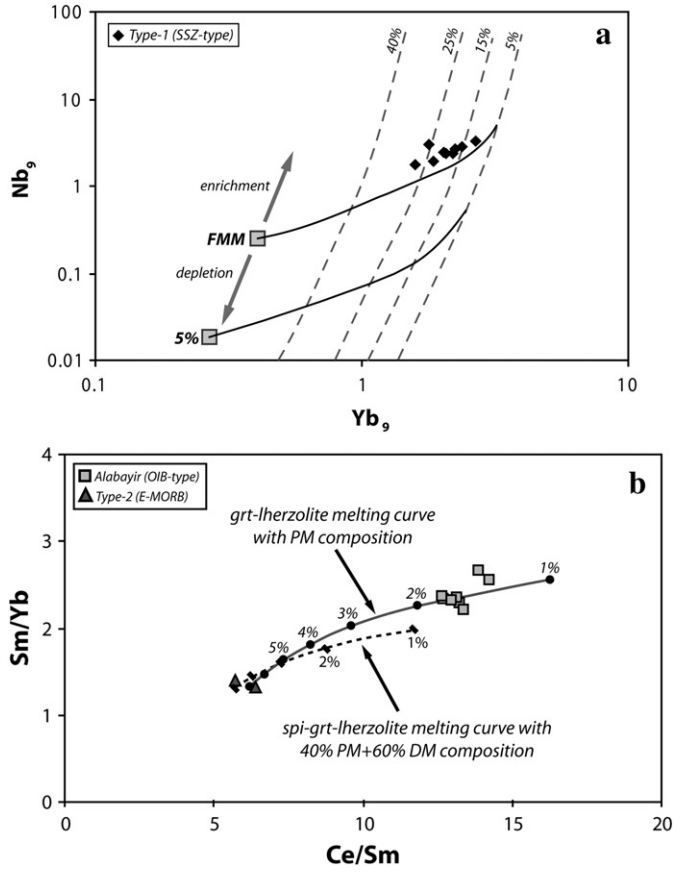

Fig. 12. a) Melting model of the SSZ-type (Type-1) samples on the basis of Nb–Yb variation. The subscript "9" denotes that the element concentrations were corrected for 9% MgO. Modelling curves are from Pearce and Parkinson (1993). The solid lines are the melting curves produced by melting of FMM and 5% depleted FMM sources. The dashed lines are the contours which joins the melt fractions that have experienced equal amount of melting. For further details, see Pearce and Parkinson (1993). b) REE-based geochemical modelling of the E-MORB (Type-2) and OIB-type (Alabayir) diabases. PM composition is from Hofmann (1988) and DM from McKenzie and O'Nions (1991). Partition coefficients are compiled from McKenzie and O'Nions (1991), Kelemen et al. (1993), Bedard (1994) and Johnson (1998). Regarding garnet–lherzolite melting curve (with PM source), the source mode is assumed to be 0.600 ol + 0.225 opx + 0.140 cpx + 0.035 grt, while the melt mode is taken as 0.030 ol + 0.040 opx + 0.540 cpx + 0.390 grt. For the spi–grt lherzolite curve (with mixed DM–PM source), the source mode is assumed to be 0.559 ol + 0.250 opx + 0.140 cpx + 0.021 grt + 0.030 spi, which melts in the proportions 0.050 ol + 0.050 opx + 0.300 cpx + 0.280 grt + 0.320 spi.

flat REE patterns of the Type-1 samples (Fig. 10a) suggests that they may have been generated in a back-arc basin (e.g. Gribble et al., 1996; Sinton et al., 2003). This is further supported by Ce/Nb, Zr/Nb and Ti/V ratios, which are generally lower in BABB relative to IAT (Fig. 13) (e.g. Fretzdorff et al., 2002; Pearce et al., 1995b; Shervais, 1982; Woodhead et al., 1993); a result related to more fertile nature of BABB over the latter. Furthermore, the Nb–Y plot indicates a FMM source, which is also in well agreement with this idea. In constrast, the depleted trace element abundances of MO-8 relative to N-MORB suggests that this sample has been generated from a pre-depleted mantle source region. Such depleted characteristics coupled with LREE depletion over HREE are typical features of island arc basalts (e.g. Pearce et al., 1995a; Peate et al., 1997; Stern et al., 2006). Indeed, this discrimination between MO-8 and the other samples can be well observed in terms of Cr–Y and Ti–V systematics; MO-8 plots in the IAT field, whereas the other Type-1 samples are rather confined to the area represented by MORB (Fig. 13).

Type-2 Mehmetalan and Mollatopuz dykes (E-MORB-type) and Alabayir dykes (OIB-type) have a different trace element systematics, and require a more enriched source region and lower degrees of partial melting. The highly fractionated REE patterns of the Alabayir suite suggest that garnet has been a residual phase during the genesis of these dykes, as further supported by the partial melting model. The less fractionated patterns shown by the Type-2 samples, however, indicate that garnet has also been involved, but a larger degree of melting is required.

E-MORB- and OIB-type basalts are typically found in tectonic settings including oceanic-islands/seamounts, continental-rifts and some flood-basalt provinces (e.g. Class et al., 1998; Furman et al., 2006; Hekinian et al., 1999). Their genesis was mostly attributed to mantle plumes, however there are also occurrences where no plume has involved (e.g. Haase and Devey, 1994). OIB-type basalts that are thought to be related to mantle plumes are known from Neo-Tethyan ocean basins, and they were generally interpreted to represent seamounts (e.g. Göncüoglu et al., 2006). This plume-related volcanism can be traced back to the Late Triassic, and was interpreted as the cause of continental break-up and subsequently opening of the northern Neotethyan basin (Göncüoglu et al., 2010). The Alabayir dykes display slightly elevated Th/Nb and Th/Yb signatures, which may reflect a subduction-derived component generated in a SSZ-type setting. Alternatively, such geochemical signatures may have been linked to a mantle-plume origin, since modern OIBs with such characteristics are known to exist (e.g. Willbold and Stracke 2006; Jackson et al. 2007).

The presence of subduction imprint observed in the Mollatopuz and Mehmetalan dykes, may imply generation in a SSZ setting. The existence of both E-MORB-type and SSZ-type samples within the

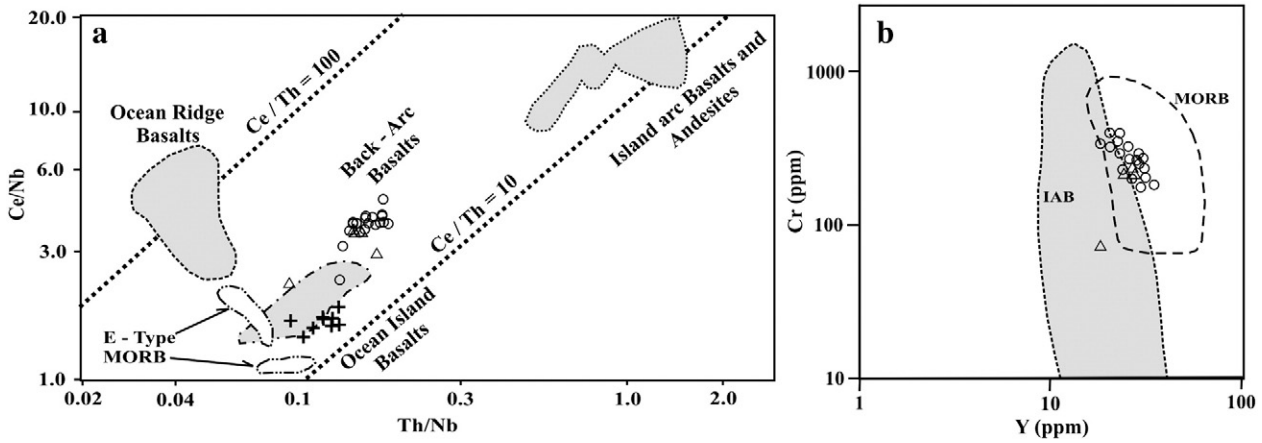

Fig. 13. Variations of a) Ce/Nb–Th/Nb (after Saunders and Tarney, 1991) and, b) Cr–Y (after Pearce et al., 1981) observed within the studied dyke suites.

same suite (Mollatopuz and Mehmetalan) strengthens this idea. Such result is further supported by the fact that both SSZ- and E-MORB-type samples have yielded similar radiometric ages (~92 and ~105 Ma, respectively). The Alabayir suite, on the other hand, only includes dykes with OIB-like characteristics; there is no SSZ-type rocks found associated with this ophiolitic suite. In spite of the absence of such association, the comparable age obtained from the Alabayir suite (~87 Ma) with those from Mollatopuz and Mehmetalan suggests that the Alabayir dykes may also have formed in a similar SSZ-type setting.

Indeed, OIB- and E-MORB-type basalts are known from arc-related settings (e.g. Fretzdorff et al., 2002; Hickey-Vargas et al., 2006; Hole et al., 1994). In intra-oceanic back-arc systems, these type of magmas can be generated from plume-contamined source regions, where the enriched plume material is brought into the depleted mantle wedge by the mantle flow around the slab via slab retreat (e.g. East Scotia Ridge, Fretzdorff et al., 2002). Furthermore, E-MORB- and OIB-type basalts with no plume involvement have also been reported from oceanic back-arcs (e.g. the West Philippine Basin, Hickey-Vargas et al., 2006). In these areas, the production of the enriched basalts has been attributed to decompression melting of a enriched mantle region in response to slab roll-back. There are some continental-arc settings where alkaline OIB-type magmas are known to be developed (e.g. Hole et al., 1994). However, considering the fact that the Alabayir dykes have formed in an oceanic environment, we preclude a continental origin for the generation of these dykes.

If the Alabayir dykes are considered to reflect a plume-related magmatism, such a plume signature may either have been acquired in an arc-basin system via mantle flow as we suggested above, or it may reflect an intra-plate mantle plume event that have developed away from the SSZ setting in which the Mehmetalan and Mollatopuz dykes were generated. Thus far, in Turkey there is no E-MORB or OIB-type magmatism known that occurred after the Early Cretaceous, which can be attributed to a mantle plume (Göncüoglu et al., 2006, 2010; Sarifakioglu et al., 2009; Sayit and Göncüoglu, 2009). If the Alabayir dykes are indeed related to such an origin, the mantle plume involvement for the early Late Cretaceous (87 Ma) OIB-type Alabayir dykes would be a new finding for southeast Anatolia. However, we find the first alternative more likely, namely generation in a SSZ-type setting, owing to the similar formation ages of the Alabayir dykes with the others.

If the enriched-type dykes were generated in a SSZ, like the depleted ones, then this event should have taken place during the closure of the Neotethys, as supported by the Ar–Ar ages indicating the Late Cretaceous time. Within the Neotethyan oceanic realm, SSZ-type basalts are known to have formed during the Early–Late Cretaceous period (Aldanmaz et al., 2008; Dilek and Furnes, 2009; Dilek et al., 1999; Göncüoglu et al., 2000; Parlak et al., 2004; Yaliniz et al., 1996). This is especially pronounced by the recent geochemical studies (e.g. Ural et al., 2010) on the basaltic rocks of the Yüksekova Complex in the western part of the Amanos–Elazig–Van suture belt around Elazig–Malatya area (Fig. 1). However, the new Ar/Ar age from Alabayir dykes confines the age of OIB-type magma emplacement to late Coniacian time. If the early Late Cretaceous age would be attributed to a mantle plume, then this suggests that the enriched dykes reflect contribution from such a plume source in their genesis, either directly or indirectly. Another alternative would be a non-plume related seamount. In this case, melting can occur within the garnet-facies mantle that contain trapped small-degree melts, and create fractionated REE patterns and enriched trace element chemistry.

6. Conclusions

Overall, our data suggest that two of the three chemical groups, including SSZ-and, E-MORB-types have been generated from a similar type of tectonic setting, namely an intra-oceanic SSZ. These distinct magmas have been created by partial melting of different source regions of the same arc-basin system. The dykes with SSZ-type geochemical signatures have been generated in a back-arc basin, involving a shallow, fertile DM source, except for MO-8 that seem to have been developed in an island-arc setting from an previously depleted mantle source. The OIB-type Alabayir dykes have either formed in a similar SSZ-environment or they reflect an unrelated intra-plate magmatism that took place in a similar time interval. Assuming a plume origin for the youngest (87.7 Ma) OIB-type dykes from the Alabayir Ophiolite our new finding in Alabayir Ophiolite would suggest that the activity of the mantle plume in the southern Neotethyan Ocean postdated the formation of SSZ-type ophiolites and hence the intra-oceanic decoupling during its closure. By this, if this preliminary data is supported by additional age determinations, our new finding may help to reconstruct the closure of the Amanos–Elazig–Van branch (Göncüoglu, 2010) of the southern Neotethys.

Our findings suggest the Mehmetalan, Mollatopuz and Alabayir ophiolites represent the remnants of the Neotethyan Amanos–Elazig–Van oceanic lithosphere. These oceanic fragments have been incorporated into the foreland flysch as allochthonous bodies from the accretionary prism during the Late Cretaceous. Our results seem to be consistent with the previous works. A number of studies suggest that the Late Cretaceous ophiolites in Anatolia have formed in an SSZ-type setting (Bagci et al., 2005; Parlak et al., 2000, 2004, 2009; Robertson, 2002; Robertson et al., 2004, 2006; Yaliniz et al., 1996, 2000). SSZ-type ophiolites are also common in the other Neotethyan ophiolites around the world (e.g. Aitchison et al., 2000; Dubois-Cote et al., 2005; Maheo et al., 2004; Pearce et al., 1981). Petrological studies carried out on the Anatolian ophiolites have revealed that these ophiolites were formed in three distinct regions of a SSZ tectonic setting, including fore-arc, island arc and back-arc (Bagci et al., 2008; Floyd et al., 2000, 2003; Göncüoglu et al., 2010; Parlak et al., 2004; Robertson et al., 2004, 2006; Sarifakioglu et al., 2009; Yaliniz et al., 1996, 2000).

Alternatively, if the new age data from other parts of the southeast Anatolian mélange complexes do not support an early Late Cretaceous plume involvement, the petrogenesis of the E-MORB and OIB-type dyke suites can be explained by small-degrees of melting of an enriched source region emplaced in the deeper levels. Such a mechanism can be achieved through a decompressional regime in the back-arc region of the northward subducting southern Neotethyan oceanic lithosphere (Göncüoglu and Turhan, 1984; Yilmaz, 1993) as a result of slab retreat. Relatively high Th/Nb ratios in some of the enriched (E-MORB and OIB) dykes can be attributed to the effect of subduction component derived from subducting slab.

Acknowledgments

This research has been supported by TUBİTAK (Project Nr CAYDAG-108Y209). The authors appreciate the useful comments and suggestions made by Editor Nelson Eby and the anonymous referees.

References

Acarlar, M., Bilgin, A., Erkal, T., Güner, E., Sen, A., Umut, M., Elibol, E., Gedik, İ., Hakyemez, Y., Uguz, F., 1991. Geology of northern and eastern part of Lake Van. General Directorate of Mineral Research and Exploration, Turkey Open File Report Nr. 9469. 94 pp. (unpublished).

Ahmad, T., Tanaka, T., Sachan, H.K., Asahara, Y., Islam, R., Khanna, P.P., 2008. Geochemical and isotopic constraints on the age and origin of the Nidar Ophiolitic Complex, Ladakh, India: implications for the Neo-Tethyan subduction along the Indus suture zone. Tectonophysics 451, 206–224.

Aitchison, J.C., Badengzhu, Davis, A.M., Liu, J., Luo, H., Malpas, J.G., McDermid, I.R.C., Wu, H., Ziabrev, S.V., Zhou, M., 2000. Remnants of a Cretaceous intra-oceanic subduction system within the Yarlung–Zangbo suture (southern Tibet). Earth and Planetary Science Letters 183, 231–244.

Akay, E., Erkan, E., Ünay, E., 1989. Stratigraphy of Mus Tertiary basin. Mineral Research and Exploration Bulletin 109, 59–77.
Aksoy, E., Tatar, Y., 1990. Stratigraphy and tectonics of E and NE part of Van. Doga Turkish Journal of Engineering and Environmental Sciences 14, 628–644.
Aldanmaz, E., Yaliniz, M.K., Güctekin, A., Göncüoglu, M.C., 2008. Geochemical characteristics of mafic lavas from the Neotethyan ophiolites in western Turkey: implications for heterogeneous source contribution during variable stages of ocean crust generation. Geological Magazine 145, 37–54.
Arculus, R.J., Powell, J.R., 1986. Source component mixing in the regions of arc magma generation. Journal of Geophysical Research 91, 5913–5926.
Austrheim, H., Prestvik, T., 2008. Rodingitization and hydration of the oceanic lithosphere as developed in the Leka ophiolite, north-central Norway. Lithos 104, 177–198.
Bagci, U., Parlak, O., Höck, V., 2005. Whole rock and mineral chemistry of cumulates from the Kizildag (Hatay) ophiolite (Turkey): clues for multiple magma generation during crustal accretion in the southern Neotethyan ocean. Mineralogical Magazine 69, 53–76.
Bagci, U., Parlak, O., Höck, V., 2008. Geochemistry and tectonic environment of diverse magma generations forming the crustal units of the Kızıldag (Hatay) ophiolite southern Turkey. Turkish Journal of Earth Sciences 17, 43–71.
Bedard, J.H., 1994. A procedure for calculating the equilibrium distribution of trace elements among the minerals of cumulate rocks, and the concentration of trace elements in the coexisting liquids. Chemical Geology 118, 143–153.
Bortolotti, V., Kodra, A., Marroni, M., Mustafa, F., Pandolfi, L., Principi, G., Saccani, E., 1996. Geology and petrology of ophiolitic sequences in the Mirdita region (northern Albania). Ofioliti 21, 3–20.
Chauvel, C., Hofmann, A.W., Vidal, P., 1992. HIMU-EM: the French Polynesia connection. Earth and Planateray Science Letters 110, 99–119.
Class, C., Goldstein, S.L., Altherr, R., Bachelery, P., 1998. The process of plume-lithosphere interactions in the ocean basins—the case of Grande Comore. Journal of Petrology 39, 881–903.
Class, C., Miller, D.M., Goldstein, S.L., Langmuir, C.H., 2000. Distinguishing melt and fluid subduction components in Umnak Volcanics, Aletuian Arc. Geochemistry, Geophysics, Geosystems 1 1999GC000010, 34 pp..
Colakoglu, A.R., 2010. Investigation of geological characteristics and Platinum Group Element (PGE) contents of Van-Özalp region chromite deposits. TUBITAK Report Nr:108Y209. 105 pp. (unpublished).
Colakoglu, A.R., Arehart, B.G., 2010. The petrogenesis of Saricimen (Caldiran-Van) quartz monzodiorite: implication for initiation of magmatism (Late middle Miocene) in the east Anatolian collision zone, Turkey. Lithos 119, 607–620.
Coleman, R.G., 1967. Low-temperature reaction zones and alpine ultramafic rocks of California: Oregon, and Washington. U.S. Geological Survey Bulletin 1247, 1–49.
Demirtasli, E., Pisoni, C., 1965. Geology of Ahlat–Adilcevaz area (N Lake Van). Mineral Research and Exploration Bulletin 64, 22–36.
Dilek, Y., Furnes, H., 2009. Structure and geochemistry of Tethyan ophiolites and their petrogenesis in subduction rollback systems. Lithos 113, 1–20.
Dilek, Y., Thy, P., Hacker, B., Grundvig, S., 1999. Structure and petrology of Tauride ophiolites and mafic dyke intrusions (Turkey): implications for the Neotethyan Ocean. Geological Society of America Bulletin 111, 1192–1216.
Dubois-Cote, V., Hebert, R., Dupuis, C., Wang, C.S., Li, Y.L., Dostal, J., 2005. Petrological and geochemical evidence for the origin of the Yarlung Zangbo ophiolites, southern Tibet. Chemical Geology 214, 265–286.
Dupuis, C., Hebert, R., Dubois-Cote, V., Wang, C.S., Li, Y.L., Li, Z.J., 2005. Petrology and geochemistry of mafic rocks from mélange and flysch units adjacent to the Yarlung Zangbo Suture zone, southern Tibet. Chemical Geology 214, 287–308.
Elliott, T., Plank, T., Zindler, A., White, W., Bourdon, B., 1997. Element transport from slab to volcanic front at the Mariana arc. Journal of Geophysical Research 102, 14991–15019.
Elmas, A., 1992. Geological investigation of Ercek Lake (Van) area. Unpublished Ph.D. thesis, University of Istanbul, 372 pp.
Elmas, A., Yilmaz, Y., 2003. Development of an oblique subduction zone—tectonic evolution of the Tethys suture zone in Southeast Turkey. International Geology Review 45, 827–840.
Elthon, D., 1979. High magnesia liquids as the parental magma for ocean floor basalts. Nature 278, 514–518.
Ewart, A., Bryan, W.B., Chappel, B.W., Rudnick, R.L., 1994a. Regional geochemistry of the Lau–Tonga arc and backarc systems. In: Hawkins, J.W., Parson, L.M., Allan, J.F., et al. (Eds.), Proceedings Ocean Drilling Programme, Scientific Results, 135, pp. 385–425.
Ewart, A., Hergt, J.M., Hawkins, J.W., 1994b. Major element, trace element, and isotope (Pb, Sr, and Nd) geochemistry of site 839 basalts and basaltic andesites: implications for arc volcanism. In: Hawkins, J.W., Parson, L.M., Allan, J.F., et al. (Eds.), Proceedings Ocean Drilling Programme, Scientific Results, 135, pp. 519–531.
Floyd, P.A., Winchester, J.A., 1975. Magma type and tectonic setting discrimination using immobile elements. Earth and Planetary Science Letters 27, 211–218.
Floyd, P.A., Göncüoglu, M.C., Winchester, J.A., Yaliniz, M.K., 2000. Geochemical character and tectonic environment of Neotethyan ophiolitic fragments and metabasites in the Central Anatolian Crystalline Complex, Turkey. In: Bozkurt, E., Winchester, J.A., Piper, J.D.A. (Eds.), Tectonics and Magmatism in Turkey and the Surroundings Area: Geological Society London, Special Publication, 173, pp. 183–202.
Floyd, P.A., Özgül, L., Göncüoglu, M.C., Yaliniz, M.K., Winchester, J.A., 2003. Metabasite blocks from the Kocyaka HP-LT metamorphic rocks, Konya, Central Anatolia: geochemical evidence for an arc–backarc pair? Turkish Journal of Earth Sciences 12, 157–174.
Fretzdorff, S., Livermore, R.A., Devey, C.W., Leat, P.T., Stoffers, P., 2002. Petrogenesis of the back-arc East Scotia Ridge, South Atlantic Ocean. Journal of Petrology 43, 1435–1467.
Frost, R.B., Beard, A.S., 2007. On silica activity and serpentinization. Journal of Petrology 48, 1351–1368.
Furman, T., Bryce, J., Rooney, T., Hanan, B., Yirgu, G., Ayalew, D., 2006. Heads and tails: 30 million years of the Afar plume. In: Yirgu, G., Ebinger, C.J., Maguire, P.K.H. (Eds.), The Afar Volcanic Province within the East African Rift System: Geological Society London Special Publications, 259, pp. 95–119.
Göncüoglu, M.C., 2010. Introduction to the Geology of Turkey: Geodynamic Evolution of the Pre-Alpine and Alpine Terranes. MTA Monographs Series. ISBN 978-605-4075-74, 66 pp.
Göncüoglu, M.C., Turhan, N., 1984. Geology of the Bitlis Metamorphic Belt. In: Tekeli, O., Göncüoglu, M.C. (Eds.), International Symposium on the Geology of the Taurus Belt, Proceedings, pp. 237–244.
Göncüoglu, M.C., Dirik, K., Kozlu, H., 1997. Pre-Alpine and Alpine terranes in Turkey: explanatory notes to the terrane map of Turkey. Annales Géologiqué de Pays Hellenique 37, 515–536.
Göncüoglu, M.C., Turhan, N., Sentürk, K., Özcan, A., Uysal, S., 2000. A geotraverse across NW Turkey: tectonic units of the Central Sakarya region and their tectonic evolution. In: Bozkurt, E., Winchester, J., Piper, J.A. (Eds.), Tectonics and Magmatism in Turkey and the Surrounding Area: Geological Society of London Special Publication, 173, pp. 139–161.
Göncüoglu, M.C., Yaliniz, M.K., Tekin, U.K., 2006. Geochemistry, tectono-magmatic discrimination and radiolarian ages of basic extrusives within the Izmir-Ankara Suture Belt (NW Turkey): time constraints for the Neotethyan evolution. Ofioliti 31, 25–38.
Göncüoglu, M.C., Sayit, K.U., Tekin, K., 2010. Oceanization of the northern Neotethys: geochemical evidence from ophiolitic melange basalts within the Izmir–Ankara suture belt, NW Turkey. Lithos 116, 175–187.
Gribble, R.F., Stern, R.J., Bloomer, S.H., Stuben, D., O'Hearn, T., Newman, S., 1996. MORB and subduction components interact to generate basalts in the southern Mariana Trough back-arc basin. Geochimica et Cosmochimica Acta 60, 2153–2166.
Günay, K., 2011. Geology, petrology, and chrome ores of Van-Özalp area ophiolites (East-Turkey). Ph.D. thesis, Yuzuncu Yil University, Institute of Science, 250 pp. (Unpublished).
Haase, K.M., Devey, C.W., 1994. The petrology and geochemistry of Vesteris Seamount, Greenland Basin—an intraplate alkaline volcano of non-plume origin. Journal of Petrology 35, 295–328.
Hart, S.R., Davis, K.E., 1978. Nickel partitioning between olivine and silicate melt. Earth and Planetary Science Letters 40, 203–219.
Hekinian, R., Stoffers, P., Ackermand, D., Revillon, S., Maia, M., Bohn, M., 1999. Ridge-hotspot interaction: the Pacific-Antarctic Ridge and the foundation seamounts. Marine Geology 160, 199–223.
Hickey-Vargas, R., Savov, I.P., Bizimis, M., Ishii, T., Fujioka, 2006. Origin of diverse geochemical signatures in igneous rocks from the West Philippine Basin: implications for tectonic models. In: Christie, D.M., Fisher, C.R., Lee, S.-M., Givens, S. (Eds.), Back-Arc Spreading Systems: Geological, Biological, Chemical, and Physical Interactions, AGU, Geophysical Monographs, 166, pp. 287–303.
Hofmann, A.W., 1988. Chemical differentiation of the Earth: the relationship between mantle, continental crust, and oceanic crust. Earth and Planetary Science Letters 90, 297–314.
Hole, M.J., Saunders, A.D., Rogers, G., Sykes, M.A., 1994. The relationship between alkaline magmatism, lithospheric extension and slab window formation along continental destructive plate margins. In: Smellie, J.L. (Ed.), Volcanism Associated with Extension at Consuming Plate Margins: Geological Society, London, Special Publications, 81, pp. 265–285.
Jackson, M.G., Kurz, M.D., Hart, S.R., Workman, R.K., 2007. New Samoan lavas from Ofu Island reveal a hemispherically heter geneous high 3He/4He mantle. Earth and Planetary Science Letters 264, 360–374.
Johnson, K.T.M., 1998. Experimental determination of partition coefficients for rare earth and high-field-strength elements between clinopyroxene, garnet, and basaltic melt at high pressures. Contributions to Mineralogy and Petrology 133, 60–68.
Kelemen, P.B., Shimizu, N., Dunn, T., 1993. Relative depletion of niobium in some arc magmas and the continental crust: partitioning of K, Nb, La and Ce during melt/rock reaction in the upper mantle. Earth and Planetary Science Letters 120, 111–134.
Keskin, M., 2005. Domal uplift and volcanism in a collision zone without a mantle plume: evidence from Eastern Anatolia. www.MantlePlumes.org. 38 pp.
Ketin, I., 1977. A short explanation about the results of geological observations at the area between Lake Van and Iran boundary. Mineral Research Exploration Bulletin 20, 79–85.
Maheo, G., Bertrand, H., Guillot, S., Villa, I.M., Keller, F., Capiez, P., 2004. The South Ladakh ophiolites (NW Himalaya, India): an intra-oceanic tholeiitic arc origin with implication for the closure of the Neo-Tethys. Chemical Geology 203, 273–303.
McKenzie, D., O'Nions, R.K., 1991. Partial melt distributions from inversion of rare earth element concentrations. Journal of Petrology 32, 1021–1091.
MTA, 2007. 1.100 000 scaled geology maps of Turkey Sheet Van. General Directorate of Mineral Research and Exploration, Ankara.
Murton, B.J., 1989. Tectonic controls on boninite genesis. In: Saunders, A.D., Norry, M.J. (Eds.), Magmatism in the Ocean Basins: Geological Society London. Special Publications, 42, pp. 347–377.
Parlak, O., Höck, V., Delaloye, M., 2000. Suprasubduction zone origin of the Pozanti–Karsanti ophiolite (southern Turkey) deduced from whole-rock and mineral chemistry of the gabbroic cumulates. In: Bozkurt, E., Winchester, J., Piper, J.A. (Eds.), Tectonics and Magmatism in Turkey and the Surrounding Area: Geological Society of London Special Publication, 173, pp. 219–234.
Parlak, O., Höck, V., Kozlu, H., Delaloye, M., 2004. Oceanic crust generation in an island arc tectonic setting, SE Anatolian orogenic belt (Turkey). Geological Magazine 141, 583–603.

Parlak, O., Rizaoglu, T., Bagci, U., Karaoglan, F., Höck, V., 2009. Tectonic significance of the geochemistry and petrology of ophiolites in southeast Anatolia, Turkey. Tectonophysics 473, 173–187.
Pearce, J.A., 1983. The role of sub-continental lithosphere in magma genesis at destructive plate margins. In: Hawkesworth, C.J., Norry, M.J. (Eds.), Continental Basalts and Mantle Xenoliths, pp. 230–249.
Pearce, J.A., Cann, J.R., 1973. Tectonic setting of basic volcanic rocks determined using trace element analyses. Earth and Planetary Science Letters 19, 290–300.
Pearce, J.A., Parkinson, I.J., 1993. Trace element models for mantle melting: application to volcanic arc petrogenesis. In: Prichard, H.M., Alabaster, T., Harris, N.B.W., Neary, C.R. (Eds.), Magmatic Processes and Plate Tectonics: Geological Society London, Special Publications, 76, pp. 373–403.
Pearce, J.A., Peate, D.W., 1995. Tectonic implications of the composition of volcanic arc magmas. Annual Review of Earth and Planetary Sciences 23, 251–285.
Pearce, J.A., Alabaster, T., Shelton, A.W., Searle, M.P., 1981. The Oman ophiolite as a Cretaceous arc–basin complex: evidence and implications. Philosophical Transactions of the Royal Society of London A 300, 299–317.
Pearce, J.A., Lippard, S.J., Roberts, S., 1984. Characteristics and tectonic significance of supra-subduction zone ophiolites. In: Kokelaar, B.P., Howells, M.F. (Eds.), Marginal Basin Geology: Geological Society London, Special Publications, 16, pp. 77–94.
Pearce, J.A., Baker, P.E., Harvey, P.K., Luff, I.W., 1995a. Geochemical evidence for subduction fluxes, mantle melting and fractional crystallization beneath the South Sandwich Island Arc. Journal of Petrology 36, 1073–1109.
Pearce, J.A., Ernewein, M., Bloomer, S.H., Parson, L.M., Murton, B.J., Johnson, L.E., 1995b. Geochemistry of Lau Basin volcanic rocks: influence of ridge segmentation and arc proximity. In: Smellie, J.L. (Ed.), Volcanism Associated with Extension at Consuming Plate Margins: Geological Society London, Special Publications, 81, pp. 53–75.
Peate, D.W., Pearce, J.A., Hawkesworth, C.J., Colley, H., Edwards, C.M.H., Hirose, K., 1997. Geochemical variations in Vanuatu arc lavas: the role of subducted material and a variable wegde composition. Journal of Petrology 38, 1331–1358.
Perincek, D., 1990. Stratigraphy of the Hakkari province, Southeast Turkey. Bulletin of the Turkish Association of Petroleum Geologists 2, 21–68.
Robertson, A.H.F., 2002. Overview of the genesis and emplacement of Mesozoic ophiolites in the Eastern Mediterranean Tethyan region. Lithos 65, 1–67.
Robertson, A.H.F., 2006. Contrasting modes of ophiolite emplacement in the Eastern Mediterranean region. In: Gee, D., Stephenson, R.A. (Eds.), European Lithosphere Dynamics: Geological Society of London, Memoirs, 32, pp. 233–256.
Robertson, A.H.F., Dixon, J.E., 1984. Introduction: aspects of the geological evolution of the Eastern Mediterranean. In: Dixon, J.E., Robertson, A.H.F. (Eds.), The Geological Evolution of the Eastern Mediterranean: Geological Society London, Special Publication, 17, pp. 1–74.
Robertson, A.H.F., Ustaömer, T., Pickett, E.A., Collins, A.S., Andrew, T., Dixon, J.E., 2004. Testing models of Late Palaeozoic–Early Mesozoic orogeny in Western Turkey: support for an evolving open-Tethys model. Journal of the Geological Society of London 161, 501–511.
Robertson, A.H.F., Ustaömer, T., Ünlügenc, Ü.C., Parlak, O., Tasli, K., Inan, N., 2006. The Berit transect of the Tauride thrust belt, S Turkey: Late Cretaceous–Early Tertiary accretionary and collisional processes related to the South-Neotethys. Journal of Asian Earth Sciences 27, 108–145.
Robertson, A.H.F., Parlak, O., Rizaoglu, T., Unlugenc¸ U., Inan, N., Tasli, K., Ustaomer, T., 2007. Tectonic evolution of the South Tethyan Ocean: evidence from the Eastern Taurus Mountains (Elazig region, SE Turkey). In: Ries, A.C., Butler, R.W.H., Graham, R.H. (Eds.), Deformation of the Continental Crust: The Legacy of Mike Coward: Geological Society, London, Special Publication, 272, pp. 231–270.
Saccani, E., Photiades, A., 2005. Petrogenesis and tectonomagmatic significance of volcanic and subvolcanic rocks in the Albanide–Hellenide ophiolitic mélanges. The Island Arc 14, 494–516.
Sarifakioglu, E., Öze, H., Winchester, J.A., 2009. Petrogenesis of the Refahiye ophiolite and its tectonic significance for Neotethyan ophiolites along the İzmir–Ankara–Erzincan suture zone. Turkish Journal of Earth Sciences 18, 187–207.
Saunders, A.D., Tarney, J., 1991. Back-arc basins. In: Floyd, P.A. (Ed.), Oceanic Basalts. Blackie and Son, London, pp. 219–263.
Sayit, K., Göncüoglu, M.C., 2009. Geochemistry of mafic rocks of the Karakaya Complex, Turkey: evidence for plume-involvement in the extensional oceanic regime during Middle–Late Triassic. International Journal of Earth Sciences 98, 367–385.
Sayit, K., Göncüoglu, M.C., Furman, T., 2010. Petrological reconstruction of Triassic seamounts/oceanic islands within the Palaeotethys: geochemical implications from the Karakaya subduction/accretion complex, Northern Turkey. Lithos 119, 501–511.
Senel, M., Ercan, T., 2002. Geological map of Turkey, 1.500,000, Van Sheet: General Directorate of Mineral Research and Exploration, Ankara, 2nd ed. .
Senel, M., Acarlar, M., Cakmakoglu, A., Erkanol, D., Taskiran, M., A., Ulu, Ü., Ünal, M., F., Örcen, S., Yildirim, H., Dager, Z., 1984. Özalp (Van)—The geology of the area between Özalp (Van)–Iran boundary. General Directorate of Mineral Research and Exploration Open File Report Nr. 663, 83pp (unpublished).
Sengör, A.M.C., Yilmaz, Y., 1981. Tethyan evolution of Turkey: a plate tectonic approach. Tectonophysics 75, 181–241.
Sengör, A.M.C., Özeren, M.S., Keskin, M., Sakinc, M., Özbakir, A.D., Kayan, I., 2008. Eastern Turkish high plateau as a small Turkic-type orogen: implications for post-collisional crust-forming processes in Turkic-type orogens. Earth-Science Reviews 90, 1–48.
Shervais, J.W., 1982. Ti–V plots and the petrogenesis of modern and ophiolitic lavas. Earth and Planetary Science Letters 59, 101–118.
Sinton, J.M., Ford, L.L., Chappell, B., McCulloch, M.T., 2003. Magma genesis and mantle heterogeneity in the Manus Back-Arc Basin, Papua New Guinea. Journal of Petrology 44, 159–195.
Spear, F.S., 1981. An experimental study of hornblende stability and compositional variability in amphibolite. American Journal of Science 281, 697–734.
Stern, R.J., Kohut, E., Bloomer, S.H., Leybourne, M., Fouch, M., Vervoort, J., 2006. Subduction factory processes beneath the Guguan cross-chain, Mariana Arc: no role for sediments, are serpentinites important? Contributions to Mineralogy and Petrology 151, 202–221.
Sun, S.S., McDonough, W.F., 1989. Chemical and isotopic systematics of oceanic basalts: implications for mantle composition and processes. In: Saunders, A.D., Norry, M.J. (Eds.), Magmatism in Ocean Basins: Geological Society of London Special Publications, 42, pp. 313–345.
Tsikouras, B., Karipi, S., Rigopoulos, I., Perraki, M., Pomonis, P., Hatzipanagiotou, K., 2009. Geochemical processes and petrogenetic evolution of rodingite dykes in the ophiolite complex of Othrys (Central Greece). Lithos 113, 540–554.
Ural, M., Kürüm, S., Arslan, M., Göncüoglu, M.C., Tekin, U.K., 2010. Petrographical and petrochemical features of Upper Cretaceous pillow lavas from Elazig and Malatya areas, SE Turkey. Geophysical Research Abstracts 12, 2010–11662 EGU.
Willbold, M., Stracke, A., 2006. Trace element composition of mantle end members:implications for recycling of oceanic and upper and lower continental crust. Geochemistry Geophysics Geosystems 7, Q04004. doi:10.1029/2005GC001005.
Winchester, J.A., Floyd, P.A., 1977. Geochemical discrimination of different magma series and their differentiation products using immobile elements. Chemical Geology 20, 325–343.
Woodhead, J., Eggins, S., Gamble, J., 1993. High field strength and transition element systematics in island arc and back-arc basin basalts: evidence for multi-phase melt extraction and a depleted mantle wedge. Earth and Planetary Science Letters 114, 491–504.
Workman, R.K., Hart, S.R., Jackson, M., Regelous, M., Farley, K.A., Blusztajn, J., Kurz, M., Staudigel, H., 2004. Recycled metasomatized lithosphere as the origin of the Enriched Mantle II (EM2) end-member: evidence from the Samoan Volcanic Chain. Geochemistry, Geophysics, Geosystems 5 (Q04008) 44 pp..
Yaliniz, M.K., Floyd, P.A., Göncüoglu, M.C., 1996. Subrasubduction zone ophiolites of Central Anatolia: geochemical evidence from the Sarikaraman ophiolite, Aksaray, Turkey. Mineralogical Magazine 60, 697–710.
Yaliniz, M.K., Göncüoglu, M.C., Floyd, P.A., 2000. Geochemistry of volcanic rocks from the Cicekdag Ophiolite, Central Anatolia, Turkey, and their inferred tectonic setting within the northern branch of the Neotethyan ocean. In: Bozkurt, E., Winchester, J., Piper, J.A. (Eds.), Tectonics and Magmatism in Turkey and the Surrounding Area: Geological Society of London Special Publication, 173, pp. 203–218.
Yigitbas, E., Yilmaz, Y., 1996. New evidence and solution to the Maden complex controversy of the Southeast Anatolian orogenic belt (Turkey). Geologische Rundschau 85, 250–263.
Yilmaz, Y., 1993. New evidence and model on the evolution of the Southeast Anatolia Orogen. Geological Society of American Bulletin 105, 251–271.
Yilmaz, Y., Saroglu, F., Güner, Y., 1987. Initiation of the neomagmatism in East Anatolia. Tectonophysics 134, 177–199.